THE LARGE-SCALE SEPARATION OF PEROXISOMES, MITOCHONDRIA, AND LYSOSOMES FROM THE LIVERS OF RATS INJECTED WITH TRITON WR-1339

Improved Isolation Procedures, Automated Analysis, Biochemical and Morphological Properties of Fractions

FEDERICO LEIGHTON, BRIAN POOLE, HENRI BEAUFAY, PIERRE BAUDHUIN, JOHN W. COFFEY, STANLEY FOWLER, and CHRISTIAN DE DUVE

From The Rockefeller University, New York, 10021. Dr. Leighton's present address is Department of Pathological Physiology, Catholic University of Chile, Santiago, Chile. Dr. Beaufay's present address is Laboratoire de Chimie Physiologique, University of Louvain, Belgium. Dr. Coffey's present address is Department of Psychiatry and Neurology, Tulane University School of Medicine, New Orleans, Louisiana

ABSTRACT

Improved, largely automated methods are described for the purification and analysis o peroxisomes, lysosomes, and mitochondria from the livers of rats injected with Triton WR-1339. With these new methods, it has become possible to obtain, in less than 6 hr and with reliable reproducibility, mitochondria practically free of contaminants, as well as the rarer cytoplasmic particles in amounts (about 100 mg of protein) and in a state of purity (95%) that make them suitable for detailed biochemical studies. The results obtained so far on these preparations have made more conclusive and precise previous estimates of the biochemical and morphological properties of the three groups of cytoplasmic particles. In addition, peroxisomes were found to contain essentially all the L-α-hydroxy acid oxidase of the liver, as well as a small, but significant fraction of its NADP-linked isocitrate dehydrogenase activity. Another small fraction of the latter enzyme is present in the mitochondria, the remainder being associated with the cell sap. The mitochondrial localization of the metabolically active cytoplasmic DNA could be verified. The relative content of the fractions in mitochondria, whole peroxisomes, peroxisome cores, lysosomes, and endoplasmic reticulum was estimated independently by direct measurements on electron micrographs, and by linear programming (based on the assumption that the particles are biochemically homogeneous) of the results of enzyme assays. The two types of estimates agreed very well, except for one fraction in which low cytochrome oxidase activity was associated with mitochondrial damage.

INTRODUCTION

At present, the only convenient method for separating rat liver peroxisomes and lysosomes from each other and from mitochondria is that based on the finding by Wattiaux and coworkers

(50, 51) that pretreatment of the animals with Triton WR-1339 causes a considerable and selective decrease in the equilibrium density of lysosomes in a sucrose gradient. We have scaled up this method and automated as much as was feasible all the operations, analytical controls, and computations involved in it, in order to have available a workable tool for the regular isolation of the rarer subcellular particles in relatively large amounts and in an acceptable state of purity. The present paper gives a critical account of the various techniques that have been worked out, together with a reappraisal of the properties of the particles as they can be deduced from the enzymic and morphological characteristics of the purified fractions. Subsequent papers will deal with their biochemical composition and metabolic properties, and with the turnover rate of their constituents.

MATERIALS AND METHODS

Preparative Procedures

14 female Sprague-Dawley rats weighing about 200 g are used for each preparation. Females were chosen because of the lower content of their liver in soluble catalase (1). 3½ days before being killed, the animals are injected intraperitoneally with Triton WR-1339 at the dosage of 85 mg per 100 g body weight. They are fasted overnight, and then killed by decapitation and bled.

For want of a satisfactory method for large-scale homogenization, we have found it preferable to handle each liver separately. The animals are killed at 3-min intervals, and the liver is quickly taken out, immersed in a tared beaker containing ice-cold 0.25 M sucrose, weighed, minced finely with sharp blades, and homogenized with approximately 20 ml of 0.25 M sucrose containing 0.1% of ethanol to prevent the formation of the inactive catalase compound II (14). Homogenization is carried out in a smooth-walled glass tube fitted with a teflon pestle (manufactured by A. H. Thomas Co., Philadelphia). The pestle is driven at about 1,000 rpm by a fixed hand drill operated by a foot switch. The tube, maintained in a plastic beaker containing a mixture of crushed ice and water, is pushed upward until all the tissue has been forced above the pestle, and then lowered. In this operation, which is performed only once on each liver, moderate pressure is applied to the homogenizer for the purpose of avoiding the excessive shearing forces generated by high vertical velocity gradients.

The pooled homogenates, containing a total of 80–100 g of liver in about 400 ml, are distributed in 12 tubes of the No. 30 rotor of the Spinco model L-HV preparative ultracentrifuge, and then subjected to an integrated force of 24,400 g-min.[1] After centrifugation, as much of the supernatant as can be removed without loss of sedimented particles is poured off. The sediments, which include unbroken cells, connective tissue fragments, erythrocytes, gross cell debris, cell membranes, most of the nuclei, and a large proportion of the mitochondria, together with smaller amounts of lysosomes, peroxisomes, and microsomes, are detached with a glass rod, combined in pairs, and rehomogenized as described above with enough sucrose-ethanol solution to make a total volume of about 35 ml. The resuspended sediments are centrifuged in six tubes and the supernatants decanted, as in the first operation. The combined sediments are homogenized once again and made up to a volume of 5 ml per g of liver processed. This fraction, which corresponds essentially to a combination of the N and M fractions of de Duve et al. (21), is labeled ν and kept for control enzyme analyses.

The combined supernatants are mixed, and their total volume is recorded. A small sample, labeled ϵ, is kept for analysis, and the remainder is distributed in 12 tubes of the No. 30 rotor and subjected to an integrated force of 342,000 g-min.[1] The supernatant and pink fluffy layer are removed as thoroughly as possible by suction. The sediments are gently worked to a smooth paste against the wall of the tubes by means of a thick glass rod, resuspended in sucrose-ethanol, and recombined in a total of three tubes for centrifugation under the same conditions. After removal of

[1] Our centrifugation conditions are expressed in integrated form, rather than in the conventional terms of x min at y g, because we operate in such a manner as to take maximum advantage of the force developed during acceleration and deceleration. The g-min integral is related to the time integral of the squared angular velocity

$$W = \int_0^t \omega^2 \, dt \tag{19}$$

by the expression:

$$g\text{-min} = W \times \frac{R_{av}}{981 \times 60}$$

in which R_{av} is the radial distance of the middle of the column of fluid during centrifugation, therefore depending on the degree of filling of the tubes. The conditions of speed and time necessary to produce a given value of W by a simple up-and-down run, with only a minimum time at plateau speed, are determined by a preliminary calibration of the centrifuge. They depend on the type of rotor used and on the load put on the rotor.

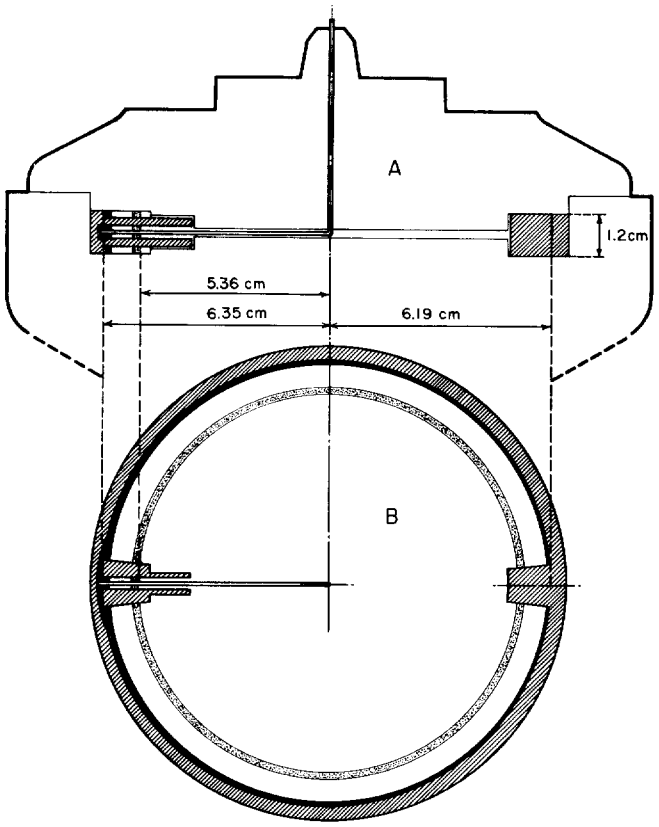

FIGURE 1 Shape of density-gradient centrifugation cell and initial disposition of layers. *A*, axial cross-section. *B*, transverse cross-section. For further details, see Beaufay (8). Cross-hatching: plastic rotor lining. Stippling: initial sample layer. White: density gradient. Black: cushion.

the supernatants together with the remainder of the fluffy layer, the sediments are transferred to one of the tubes with addition of a minimum amount of sucrose-ethanol solution and rehomogenized with a loose-fitting teflon ball driven by a motor, to make a thick suspension of 8.5–9.0 ml total volume. This fraction, which, except for a somewhat higher content of mitochondria, is equivalent to the L fraction of de Duve et al. (21), is labeled λ. It is weighed and its volume is calculated by dividing the weight by 1.08, the measured density of such suspensions. The combined supernatants, which include the microsomal and soluble fractions, are made up to 10 ml per g of liver processed, mixed, and labeled ψ.

Subfractionation of the λ fraction is carried out by isopycnic centrifugation in the automatic rotor assembly designed by Beaufay (8). This equipment has the following advantages over the SW-39 swinging bucket rotor: (1) Thanks to the shape of the centrifugation cell (Fig. 1), the time necessary to achieve a given result in the new rotor is only about one-fourth that required with the SW-39 rotor running at the same speed. (2) Loading and unloading are carried out while the rotor is running, by means of a special device which can be disengaged before the rotor is accelerated to high speed and reengaged again when the rotor speed falls below 10,000 rpm; this device is operated from the outside without disturbance of the vacuum inside the centrifuge chamber. This arrangement suppresses convective artifacts associated with starting and stopping the centrifuge, and renders unnecessary the various precautions that have to be taken during acceleration and deceleration of swinging bucket rotors (19). (3) The fractions are delivered automatically into a fraction collector. (4) The rotor has a capacity of 45 ml, making a single run equivalent to three complete runs with the SW-39 rotor on a total of nine tubes.

Fig. 1 illustrates the shape of the centrifugation cell and the initial disposition of the layers. The cell is a pseudo-cylindrical ring, 1.2 cm high, and delimited by two opposed half-spirals designed to allow the densest layer of fluid to spread from, and to converge toward, the point of maximal radius. A tube, serving as both inlet and outlet, descends axially and then bends at a right angle, following the direction of the longest radius and ending in a shallow groove hollowed out at midheight in the wall of the cell; this groove is covered by a lucite sleeve which forms an incomplete septum at this point. A removable device,

described in detail in Beaufay's book (8), fits hermetically on the upper cone of the rotor and provides a connection with the outside for filling and emptying. Loading of the rotor spinning at about 5,000 rpm is done in the order of increasing density by means of a multiple-syringe machine equipped with a multiway valve.

For subfractionation of the λ fraction, we inject successively: (1) 8 ml of λ fraction, containing the particles isolated from about 80 g liver; (2) a density gradient extending linearly with respect to volume between densities 1.15 and 1.27, and occupying a total volume of 26 ml; (3) a 6-ml cushion of density 1.32. The gradient is made with two simultaneously driven syringes of equal cross-section, filled with the two solutions whose composition is given in Table I. The heavy solution is driven into the syringe containing the light solution in which vigorous mechanical mixing is maintained, while this mixture of continuously increasing density is itself driven into the rotor. The solutions described in Table I are prepared by dissolving adequate amounts of sucrose in water containing 5% (w/w) of dextran-10 and 0.1% of ethanol. Dextran was included after preliminary experiments indicated that it may improve the resolution as well as the state of conservation of the peroxisomes. This effect has not been explored systematically. As mentioned above, ethanol is added to prevent catalase inactivation. As indicated in Fig. 1, the sample and gradient form initially two concentric layers, respectively 2.07 and 6.25 mm thick; the cushion fills the whole eccentric space and an additional circular layer 0.55 mm thick. Thanks to the centrifugal field, these layers spread with essentially no convective mixing.

TABLE I

Composition of Solutions Used in Fractionation

Solution	Grams per 100 g solution		
	Sucrose	Dextran-10	0.1% Ethanol in H_2O
Homogenization and differential centrifugation	8.25	—	91.75
Gradient: Light solution	30.40	3.48	66.12
Gradient: Heavy solution	53.33	2.33	44.34
Gradient: Cushion	60.00	2.00	38.00

As soon as filling is completed, the rotor is accelerated sufficiently to prevent back flow of fluid, the connecting device is disengaged, and the rotor is then accelerated further to 35,000 rpm and maintained at this speed for 37 min. After deceleration to 9,000 rpm, the connecting device is reengaged and nitrogen is injected into the rotor at a pressure of about 15 atm. Disturbance of the gradient by gas bubbles during this operation is prevented by the lucite sleeve. The pressure of the gas phase in the rotor tends to force the fluid through the tube towards the axis (see Fig. 1). As long as the rotational speed is sufficient, the centrifugal field acting on the column of fluid in the tube prevents it from reaching the axis. As the rotor is allowed to decelerate, a speed is reached at which the centrifugal field becomes insufficient to counteract the effect of the gas pressure and unloading occurs, until the pressure in the expanding gas phase becomes equal to the hydrostatic pressure in the tube. Thus, the rate of unloading is governed by the rate of deceleration, and smooth delivery at a predetermined rate can be obtained by a simple feedback device, which also operates the fraction collector (8). As a rule, some 20 2-ml fractions are collected, each corresponding to a cylindrical layer 12 mm high and about 0.5 mm thick. The fractions are collected in tared tubes and weighed. Their density is then measured by the organic solvent gradient method described by Beaufay et al. (11).

All centrifugations are carried out at a temperature near 0°. Our centrifuges are equipped with a cold trap and a diffusion pump (Spinco Model LHV), which help to maintain a high vacuum and improve the temperature stability. Between the killing of the first animal and the collection of the last fraction, the whole operation takes approximately 5½ hr.

In a number of separate experiments, lysosomes were isolated by a modification of the procedure devised by Trouet (47). A combined M + L fraction, prepared by the procedure of de Duve et al. (21) from the livers of rats injected with Triton WR-1339, is resuspended in 45.0% (w/w) sucrose (density 1.21) to a volume of 1 ml per g of liver processed. 25 ml of this suspension are layered at the bottom of a discontinuous gradient consisting of a 20-ml layer of 34.5% (w/w) sucrose (density 1.155) and a 10-ml layer of 14.3% (w/w) sucrose (density 1.06). Three such tubes, containing particles from 75 g of liver, are centrifuged for 2 hr at 25,000 rpm in the SW-25.2 rotor of the Spinco Model L2-HV preparative ultracentrifuge. The lysosomes collect at the interface

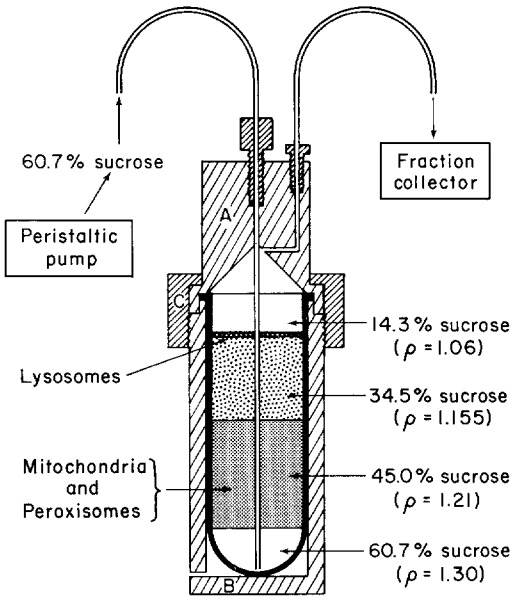

FIGURE 2 Collection of fractions separated by discontinuous gradient method of Trouet (47). Parts *A* and *B* are made of lucite and are held tightly together by means of metal screw cap *C*. Air-tight junctions are ensured by means of O-rings. Tube contents are slowly driven upward into collecting cone by injection of dense solution of sucrose. Fluorocarbon (FC-43, Fluorochemical, 3M Chemical Co., St. Paul, Minn.) may be used instead of the sucrose solution.

between the two upper layers, whereas most of the mitochondria and peroxisomes remain in the bottom layer. These fractions are recovered through a collecting cone fitted hermetically on top of the tube and traversed by a needle through which 60.7% (w/w) sucrose (density 1.30) is injected into the bottom of the tube so as to push its contents upwards (Fig. 2). The flotation procedure described has also been used for the further purification of the lysosome-rich fractions isolated in the automatic rotor. These fractions, which have an average density of about 1.12, are mixed with an equal volume of 60.7% (w/w) sucrose (density 1.30) and processed in the same way as the M + L fractions.

Biochemical Analyses

Automated or semi-automated methods were used for all routine biochemical analyses. These were performed on suitable dilutions of the fractions prepared with a solution of pH 7.6, containing 1 mM sodium bicarbonate, 1 mM EDTA, 0.1% of ethanol, and 0.01% of Triton X-100.

Time-course determinations were carried out with the Gilford Model 2000 spectrophotometer (Gilford Instrument Laboratories, Inc., Oberlin, Ohio), which provides an output voltage proportional to the absorbance, connected to a Linear/Log Varicord Model 43 recorder (Photovolt Co., New York), which offers the possibility of recording either the absorbance signal as such or its logarithm. Full advantage of this combination is taken in the assay of cytochrome oxidase, which obeys first-order kinetics with respect to cytochrome *c* (2, 16). The reaction is started by the rapid addition of 3 ml of 34 μM reduced cytochrome *c*, in 30 mM potassium phosphate buffer, pH 7.4, to 0.1 ml of enzyme. The logarithm of the absorbance at 550 mμ is recorded for 4–8 min, with oxidized cytochrome *c* present at the same concentration in the reference cuvette. The plot gives a straight line, the negative slope of which is proportional to the activity of the enzyme. When expressed in $\log_{10}$ min^{-1} and multiplied by 3.1/100, this slope gives the activity of the preparation in the units defined by Cooperstein and Lazarow (16). Substrate is added simultaneously to three cuvettes by three interlocked automatic syringes fitted directly above the sample compartment of the spectrophotometer (this device was constructed by Dr. R. L. Deter). The reaction is run at 25°.

Other spectrophotometric assays are also run with the Gilford instrument, but with direct recording of the absorbance. Urate oxidase is measured by following the decrease in absorbance at 292 mμ after addition of 3 ml of 42 μM sodium urate in 30 mM potassium phosphate buffer pH 7.4, containing 1 mM EDTA and 0.1% of Triton X-100, to 0.1 ml of enzyme (21, 40). The reaction, which is started simultaneously in three cuvettes, is run at 37°. One unit of activity corresponds to the oxidation of 1 μmole of urate per min, or to a decrease of 3.94 absorbance units per min, under the conditions described (33). If necessary (turbid enzyme suspensions), a blank is run similarly in the absence of urate.

In the assay of glutamate dehydrogenase, the increase in absorbance at 340 mμ is measured in a final volume of 2 ml containing 20 mM sodium glutamate, 1.4 mM NAD, 20 mM glycylglycine-NaOH, buffer pH 7.7, 30 mM nicotinamide, 0.4 mM NaCN, 1 mM EDTA, and 0.1% of Triton X-100 (9, 30). The reaction is run at 25°, and the readings are taken against a blank cell containing the same amount of enzyme and all reagents except NAD. One unit of activity corresponds to the reduction of 1 μmole of NAD per min, or to an increase of 3.11 absorbance units per min under the conditions described (31).

In the assay of the NADP-linked isocitrate dehydrogenase (34), a small volume of enzyme is first added with a micropipette to a mixture containing, in a final volume of 2.9 ml, 0.1 mM NADP, 34 mM potassium phosphate buffer pH 7.4, 3.3 mM $MgCl_2$, and 0.07% of Triton X-100. The absorbance at 340

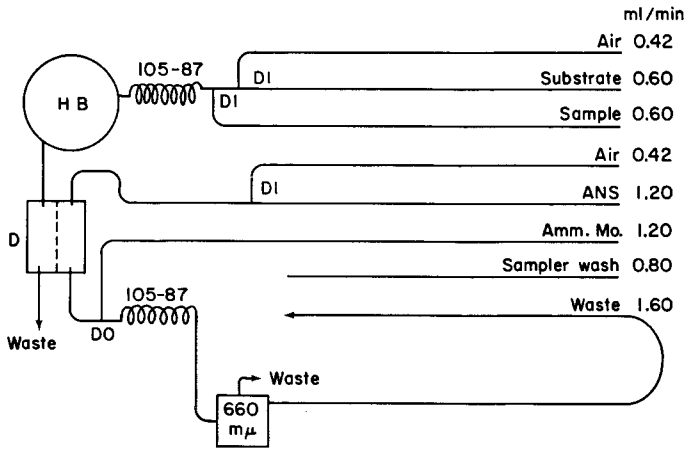

FIGURE 3 Automated phosphatase assay. *HB*, heating bath, 37°, 80-ft. coil, 1.6 mm I.D.; *D*, single dialyzer at 37°; for other symbols refer to Technicon catalogue. *Substrate* (acid phosphatase): Mixture containing, per ml, 0.2 ml of 0.5 M Na β-glycerophosphate brought to pH 5 with HCl; 0.1 ml of 1 M Na acetate-acetic acid buffer pH 5; 0.1 ml of 2% (v/v) Triton X-100; 0.6 ml of H_2O. *Substrate* (glucose-6-phosphatase): Mixture containing, per ml, 0.5 ml of 0.08 M K glucose-6-phosphate brought to pH 6.5 with HCl; 0.1 ml of 0.02 M EDTA pH 6.5; 0.2 ml of 0.2 M histidine-HCl buffer pH 6.5; 0.2 ml of 1.5% (w/v) solution of bovine serum albumin. *ANS*, freshly prepared eight-fold aqueous dilution, supplemented with 0.05% Levor (Technicon), of a 0.2% solution of aminonaphtholsulfonic acid in 1.44 M $NaHSO_3$-Na_2SO_3 (24). *Amm Mo*, fourfold dilution of 0.02 M ammonium molybdate in 5 N H_2SO_4. *Washing fluid:* 0.05% Levor (Technicon) in water. *Standard:* 1 mM KH_2PO_4 in 0.01 N H_2SO_4. Sampling rate: 30 samples per hour. Colorimetry at 660 mμ with tubular flow cell of 15 mm light path. Recording: transmission on log paper.

mμ is recorded for 1–2 min to provide a base-line, and the reaction is then started by addition of 0.1 ml of 0.2 M sodium DL-isocitrate. The change in the slope of the recording is a measure of the activity of the enzyme. The reaction is run at 30°. One unit of activity corresponds to the reduction of 1 μmole of NADP per min under the conditions described.

The other determinations were done with Technicon Auto-Analyzer units (Technicon Corp., Ardsley, N.Y.), the sampler being kept in a refrigerator. The methods were patterned after the standard assay procedures in use in the laboratory. A number of modifications were required for optimum accuracy, reproducibility, and linearity with respect to enzyme concentration.

Assays for acid phosphatase and glucose-6-phosphatase were adapted from de Duve et al. (21). Details of the method, which can be extended to other substrates, are shown in Fig. 3. After incubation of enzyme and substrate at 37° for approximately 30 min, inorganic phosphate is partially removed from the mixture by dialysis and measured according to Fiske and SubbaRow (24). The samples are run a second time with a buffer mixture containing no substrate, for determination of the enzyme blanks. This technique gave good results with acid phosphatase, but not with glucose-6-phosphatase which appears to suffer progressive surface denaturation during its flow through the system. Inactivation was largely prevented by addition of 0.3% of bovine serum albumin to the substrate mixture. However, when repeated assays were run under these conditions on the same enzyme preparation, the first activities recorded were still low, increasing progressively to reach a stable and reproducible value after the third or fourth assay, possibly owing to the formation of a protective coating on the tube walls. In view of this observation, each new cycle of glucose-6-phosphatase assays was always started with six identical samples of cytoplasmic extract diluted 300-fold. The glucose-6-phosphatase activities measured as described here represent the contributions of the specific glucose-6-phosphatase and of the unspecific acid phosphatase to the hydrolysis of glucose-6-phosphate. We have found by repeated measurements on intact preparations and on preparations in which glucose-6-phosphatase had been selectively inactivated by a 30-min incubation at pH 5 and 37° (20), that the amount of inorganic phosphate released by acid phosphatase from glucose-6-phosphate under the conditions of the glucose-6-phosphatase assay is equal to one-fifth of the amount released from β-glycerophosphate under the conditions of the acid phosphatase assay. This contribution becomes quite important in lysosome-rich

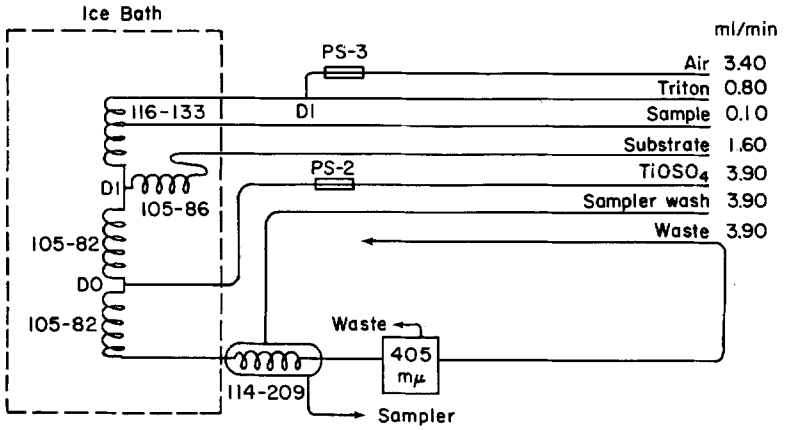

FIGURE 4 Automated catalase assay. For symbols, refer to the Technicon catalogue. *Triton,* solution of 1% Triton X-100 and of 0.33% bovine serum albumin in 2% NaCl. *Substrate:* Solution containing 0.07% of 30% H_2O_2 in 0.033 M imidazole-HCl buffer pH 7.0. *TiOSO4*: Prepared by dissolving 27 g of titanium oxysulfate in 4 liters of boiling 2 N H_2SO_4, filtering on Whatman # 42 paper after cooling, and diluting the filtrate with 2 liters of 2 N H_2SO_4. *Washing fluid:* 0.05% of BRIJ-35 (Technicon) in water. Sampling rate: 20 samples per hour. Colorimetry at 405 mμ in Beckman DB spectrophotometer with rectangular flow cell of 6-mm light path.

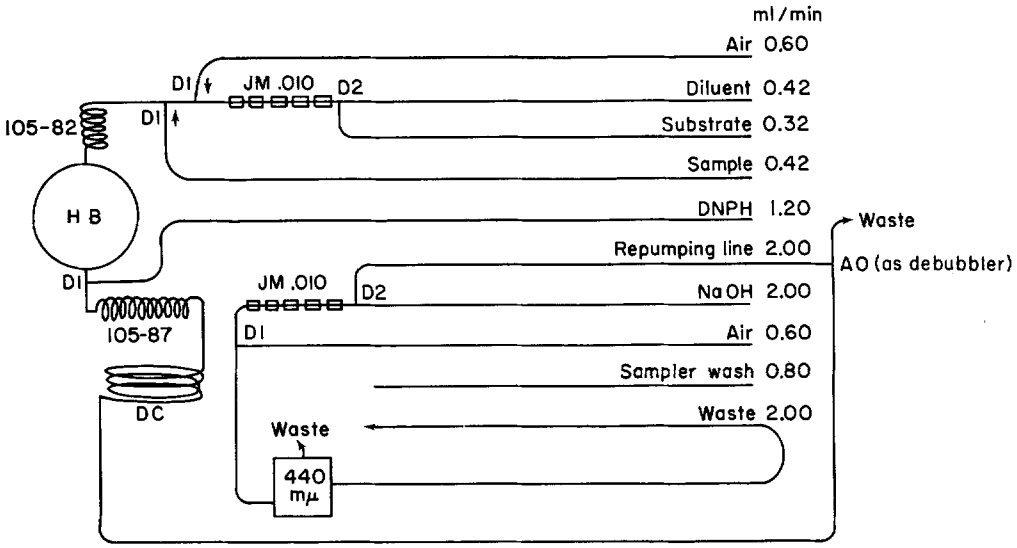

FIGURE 5 Automated assay of D-amino acid oxidase and of L-α-hydroxy acid oxidase. *HB,* heating bath, 37°, 80-ft coil, 1.6 mm I.D.; *JM.010,* jet mixer, alternate segments of tygon tubing of 0.010 and 0.0625 in. I.D.; *DC,* delay coil, 8 ft, 2 mm I.D.; other symbols refer to Technicon catalogue. *Diluent:* Freshly prepared mixture of one volume of 2% Triton X-100 with five volumes of 0.15 M sodium pyrophosphate-HCl buffer pH 8.6 containing 80 mg/l of FAD (D-amino acid oxidase), or with five volumes of 0.10 M sodium pyrophosphate-HCl buffer pH 8.0 (L-α-hydroxy acid oxidase). *Substrate:* (D-amino acid oxidase): 0.2 M D-alanine, brought to pH 8.6 with NaOH. *Substrate:* (L-α-hydroxy acid oxidase): 0.025 M sodium glycolate. *DNPH* solution of 0.01% 2,4-dinitrophenylhydrazine in 2 N HCl containing 0.2% of Triton X-100. *NaOH,* 1.5 N. *Washing fluid:* Water. *Standard:* 0.2 mM redistilled pyruvic acid (D-amino acid oxidase) or glyoxylic acid (L-α-hydroxy acid oxidase). Sampling rate: 30 samples per hour. Colorimetry at 440 mμ with tubular flow cell of 15-mm light path. Recording: transmission on log paper.

samples and may, if not corrected for, cause an overestimation of the microsomal contamination in the sample. All the glucose-6-phosphatase values given in this paper have been corrected on the basis of the acid phosphatase measurements and, therefore, refer to the true microsomal glucose-6-phosphatase. Phosphatase activities are expressed in μmoles of inorganic phosphate released per min.

Fig. 4 illustrates the automated catalase determination, which is an adaptation of the method of Chantrenne (15), as modified by Baudhuin et al. (4). Inactivation of the enzyme is prevented by addition of 0.33% of bovine serum albumin to the detergent solution used to disrupt the peroxisomes. Owing to the minuteness of the enzyme sample (0.1 ml), the inner diameter of the sample line must not, at any point, exceed 0.025 in.; otherwise, merging of the sample with washing fluid may occur. This condition applies to the sampling needle, to all connections, and to the middle arm of the first coil, which is narrowed by insertion of a segment of polyethylene tubing. After incubation for approximately 1.5 min at 0°, the hydrogen peroxide remaining in the mixture is measured as the yellow peroxytitanium sulfate complex. For the reagent blank, buffer solution is substituted for substrate during a short period before and after the assay. In rare cases, where the enzyme samples are extremely turbid, the contribution of the precipitated proteins to the absorbance at 405 mμ is determined by a second sampling cycle run with buffer alone. Since catalase obeys first order kinetics, the results are expressed as the logarithm of the ratio of the initial to the final hydrogen peroxide concentration. The unit of activity is the amount of enzyme which causes the decadic logarithm of the H_2O_2 concentration to decrease by one unit per min in a volume of 50 ml.

The method used for measuring D-amino acid oxidase and L-α-hydroxy acid oxidase is shown in Fig. 5. It is derived from the D-amino acid oxidase method of Baudhuin et al. (4) and depends on the colorimetric determination of α-keto acids as their dinitrophenylhydrazones. It can be adapted to other substrates with standardization of the corresponding hydrazones. For instance, L-lactate can be used for the assay of L-α-hydroxy acid oxidase. We prefer the optically inactive glycolate because in liver this substrate is attacked mainly by the oxidase, whereas other systems capable of oxidizing L-lactate are also present. Glycolate is also oxidized more rapidly than lactate by the liver enzyme. Good results were obtained without extraction of the dinitrophenylhydrazone. The repumping line inserted after completion of the hydrazone formation provides a stable flow rate before the addition of alkali, and a noiseless recording. Enzyme blanks are obtained by running a second cycle without substrate. The incubation time is about 30 min at 37°. Activities are expressed

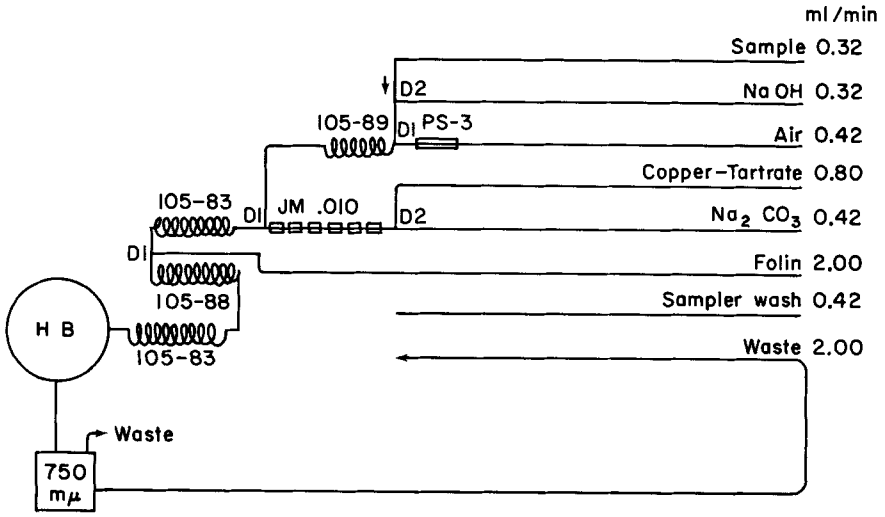

FIGURE 6 Automated protein determination. *JM.010*, jet mixer, alternate segments of tygon tubing of 0.010 and 0.0625 in. I.D.; *HB*, heating bath, 37°, 80-ft. coil, 1.6 mm I.D.; other symbols refer to Technicon catalogue. *NaOH*, 1 N. *Copper tartrate:* Solution containing 0.73 mM $CuSO_4$ and 2.6 mM sodium-potassium tartrate (less than 2 wk old). *Na_2CO_3*, 0.69 M. *Folin*, freshly prepared 12.5-fold aqueous dilution of Folin-Ciocalteu reagent. *Washing fluid:* 1% NaCl. *Standard:* 0.01% of bovine serum albumin in water. Sampling rate: 30 samples per hour. Colorimetry at 750 mμ in tubular flow-cell of 15-mm light path. Recording: transmission on log paper.

in μmoles of α-keto acid (dinitrophenylhydrazone) formed per min.

The method of Lowry et al. (36) for the determination of protein was adapted as shown in Fig. 6. Reagent concentrations and reaction times had to be modified for optimal results in a continuous flow system. Results are expressed in bovine serum albumin equivalents.

Morphological Examinations

The filtration technique described by Baudhuin et al. (6) was used with minor modifications for preparing fractions for electron microscopy. Fixation was done in two steps. The fractions were first mixed with one-fourth their volume of a solution containing 7.5% of glutaraldehyde in 0.25 M phosphate buffer pH 7.4. After 5 min, they were diluted ten-fold or more with 1.5% glutaraldehyde in 0.05 M phosphate buffer pH 7.4 to a protein concentration of about 0.5 mg per ml. This two-step technique was adopted on the assumption that fixed particles may suffer less damage from the osmotic shock associated with dilution than unfixed particles. After fixation, 0.3-ml samples of fixed suspension were filtered through Millipore membranes of 0.01-μ pore size, postfixed with osmium tetroxide, dehydrated, embedded in Epon, sectioned, and stained, exactly as described by Baudhuin et al. (6). Sections were photographed in a Siemens Elmiskop I electron microscope at 60 kv.

The relative contribution of each morphological component to the total volume of particulate matter present in a fraction was estimated on micrographs by the method of Rosiwal (37). Micrographs including the whole thickness of the pellicle were enlarged to a

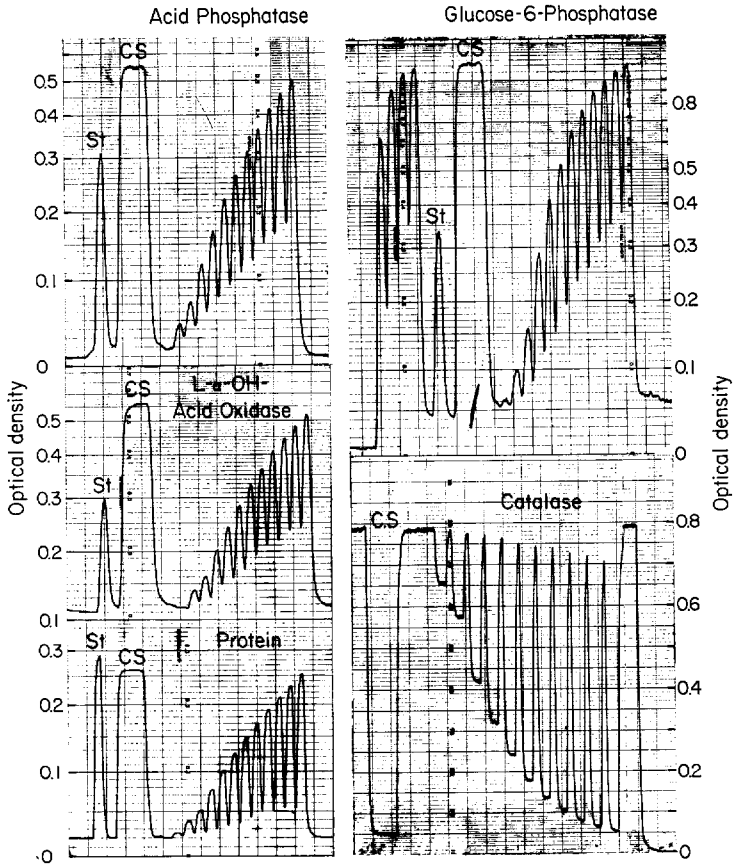

FIGURE 7 Automated biochemical assays. Experimental tracings obtained with increasing amounts of a cytoplasmic extract (see Fig. 8 for concentrations). *St*, standard. *CS*, recording obtained during continuous sampling of liver extract used; provides the plateau value corresponding to last peak and gives an idea of the washing characteristics and of the degree in which plateau is approached in each method. Glucose-6-phosphatase assay is preceded by four assays at the highest concentration used, illustrating progressive displacement of base line and peak.

final magnification of 30,000–50,000, and covered by a grid of parallel lines with a constant spacing of 20 or 30 mm, depending on the magnification. The total length of lines included within profiles of each type was measured to provide an estimate of the relative total surface area of the profiles in the section, and, therefore, of the relative total volume of the corresponding particles in the pellicle. (For a summary of grid measurement methods, see reference 44). Measurements were made on all the structures seen, except the glycogen particles present in fraction 21 (see Fig. 17 *b*); these particles were assumed to contain no protein and were, therefore, neglected for comparison with the biochemical results which were computed on a protein basis. For each fraction, the measurements were repeated on three to six micrographs representing widely spaced sections through the pellicle and covering a total area of about 500 μ^2. In agreement with previous results indicating that the filtration technique used satisfies the criterion of true random sampling (6), closely similar values were obtained for all measurements on different sections of the same pellicle.

Calculations

All the calculations and the plotting of results were performed on a CDC 160 G computer with a 165 plotter on line. Conversion of the raw data to distribution histograms was done exactly as described by Beaufay et al. (11). For density distributions, the density boundary between two adjacent fractions was taken as the weighted average of their measured densities: $(V_i\rho_j + V_j\rho_i)/(V_i + V_j)$, in which V and ρ refer to the volume and density of adjacent fractions. This assumption introduces negligible error in view of the linearity of the density gradients.

The following procedure was adopted for averaging density distribution histograms characterized by different density boundaries. Each histogram was first converted to a curve composed of successive segments of second degree functions fitted according to the following conditions: (*a*) that the integral of the curve between the fraction boundaries be equal to the proportion of the total enzyme activity present in that fraction, and (*b*) that the height of the curve at each boundary be equal to the average of the heights of the histogram bars separated by the boundary. We then integrated the complex distribution curves calculated in this manner over standard density intervals, to produce a new set of histograms with uniform density intervals, which could then be averaged directly. These calculations can be reduced to a simple conversion formula which is easily handled by the computer. This treatment is more complicated, but more rigorous than that adopted previously (12, 23). It gave sharper peaks and smaller standard deviations than the simpler averaging procedure.

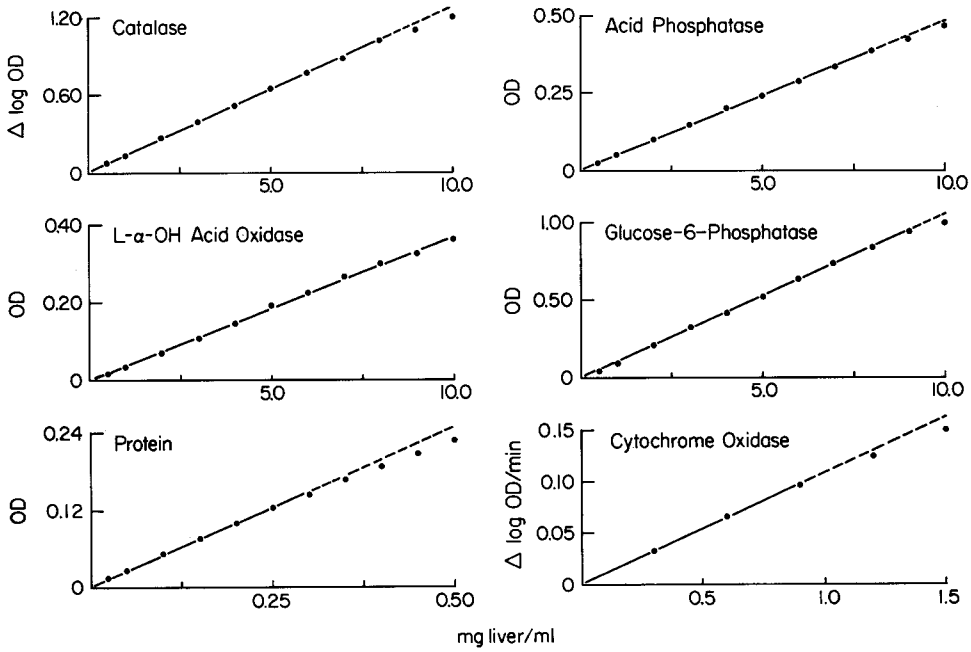

FIGURE 8 Automated biochemical assays. Results of Fig. 7 plotted as a function of concentration of cytoplasmic extract used.

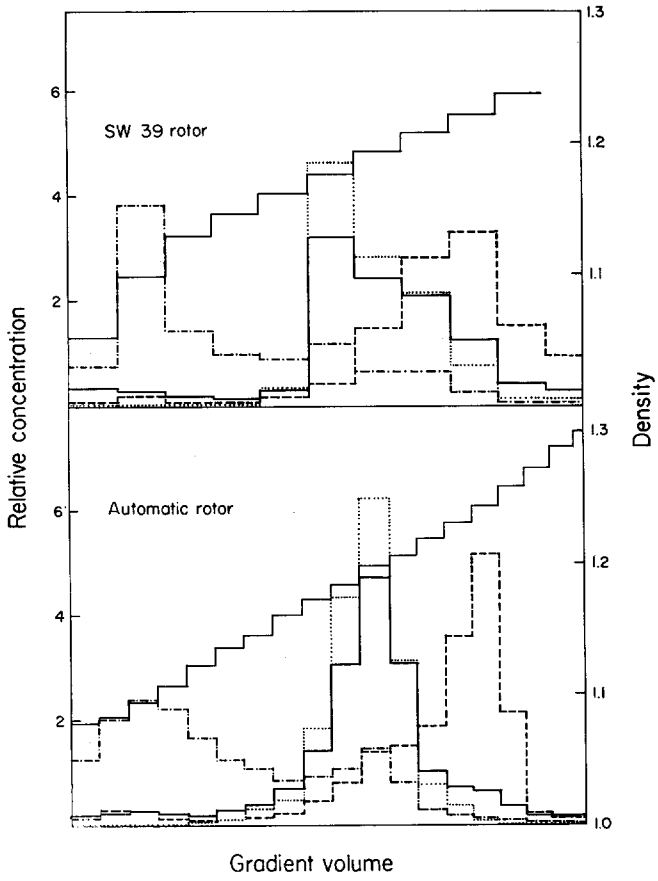

FIGURE 9 Isopycnic subfractionation of M + L fraction from rat injected with Triton WR-1339. Results obtained with SW-39 rotor (150 min at 39,000 rpm) and with automatic rotor (37 min at 35,000 rpm) on samples of the same particulate fraction. Graphs show, for each fraction, average density (thin solid line in ascending steps, right-hand ordinate) and enzyme concentration relative to concentration corresponding to uniform distribution throughout gradient (left-hand ordinate): acid phosphatase (—·—·—), cytochrome oxidase (·····), protein (thick solid line), catalase (– – –).

Materials

All chemicals were of analytical grade. Cytochrome *c* (grade VI), disodium β-glycerophosphate (grade I), dipotassium glucose-6-phosphate, FAD (grade III), β-NAD (grade III), and NADP (Sigma grade) were purchased from the Sigma Chemical Company (St. Louis). Titanium oxysulfate was obtained as "Titanium Sulfate cake C. P." from A. D. Mackay, Inc. (New York). Triton WR-1339 and Triton X-100 were obtained from Rohm and Haas (Philadelphia). Bovine serum albumin was purchased as fraction V from bovine plasma from Armour Pharmaceutical Company (Kankakee, Ill.).

RESULTS

Biochemical Assays

Fig. 7 shows a set of recordings obtained in the automated enzyme assays. Adequate resolution of adjacent fractions is achieved with only slight dilution in the peak region. The necessity of "priming" the manifold for the glucose-6-phosphatase assay is also illustrated. As indicated in Fig. 8, the results show good proportionality with enzyme concentration over a wide range. Measurements falling beyond the range of linearity were repeated with a higher dilution of enzyme. One of the numerous advantages of the automated procedures is that results become available with little delay and unsatisfactory assays are easily repeated under better conditions.

Fractionation Procedures and Enzyme Distributions

In Fig. 9 are shown the results of an early experiment in which samples of the same M + L fraction (21) were subfractionated by isopycnic density gradient centrifugation simultaneously with the SW-39 rotor (11) and with the automatic rotor. In addition to the many advantages already mentioned (see Materials and Methods), the new rotor yields the mitochondria in a narrow symmetrical band, in contrast with the SW-39

TABLE II

Results of Fractionation of Liver

Values listed are means ± standard deviation.

Enzyme	No. of experiments	Content of liver	Percentage distribution			Over-all recovery‡
		*Units/g**	*ν*	λ	*ψ*	*% of* (*ε* + *ν*)
Protein	21	260 ± 48	36.1 ± 4.3	8.1 ± 1.5	55.8 ± 3.6	97.1 ± 3.5
Acid phosphatase	21	8.9 ± 1.3	30.5 ± 5.4	18.8 ± 4.1	50.7 ± 6.3	94.6 ± 4.1
Glucose-6-phosphatase	19	13.9 ± 3.5	24.0 ± 7.3	2.4 ± 1.1	73.6 ± 7.3	100.4 ± 10.6
Cytochrome oxidase	21	23.4 ± 3.7	70.3 ± 7.9	25.9 ± 7.1	3.8 ± 1.4	90.2 ± 11.0
Glutamate dehydrogenase	1	20.2	58.4	33.0	8.6	116.4
Isocitrate dehydrogenase	3	27.6 ± 6.5	17.7 ± 4.8	6.2 ± 0.5	76.1 ± 4.9	95.4 ± 18.1
Catalase	21	45.0 ± 7.5	26.2 ± 5.8	39.0 ± 5.7	34.8 ± 4.8	94.3 ± 5.0
L-α-Hydroxy acid oxidase	10	1.14 ± 0.23	26.1 ± 3.8	32.7 ± 6.6	41.2 ± 6.1	95.6 ± 8.4
D-Amino acid oxidase	6	1.44 ± 0.23	31.7 ± 5.5	34.2 ± 3.4	34.1 ± 7.0	99.0 ± 12.3
Urate oxidase	4	3.1 ± 0.5	39.9 ± 7.0	42.5 ± 4.9	17.6 ± 3.1	77.7 ± 8.2

* Proteins are given in mg/g, enzymes in units/g.

‡ Sum of contents of ε + gradient fractions + ψ.

rotor where the distribution of cytochrome oxidase is skewed on the dense side, extending far into the peroxisome region. This difference has been essential to the successful purification of peroxisomes.

At the time of writing this report, twenty-one separations have been carried out by the new technique, with very reproducible results. The general properties of the livers and the data on the preliminary fractionation are summarized in Table II. Compared to the results of earlier determinations made on normal rats of a different strain (4, 9, 21, 41), our absolute enzyme activities are not sufficiently different to invite comment. However, the hepatic protein content of our animals is distinctly higher than the values of 200–220 mg/g (or 32–34 mg N/g) found previously. Whether the treatment with Triton WR-1339 or other factors are responsible for this difference is not known.

The λ fraction (Table II) resembles in biochemical composition an L fraction prepared according to de Duve et al. (21). It contains somewhat more protein and mitochondrial enzymes; but it has less acid phosphatase, probably because of a greater fragility of the swollen Triton-filled lysosomes. Its microsomal contamination indicated by glucose-6-phosphatase is suitably low, thanks to the thorough removal of the pink fluffy layer upon decantation. Its content in peroxisomal enzymes is comparable to that of an L fraction (4).

As reported briefly elsewhere (7), the distribution of the L-α-hydroxy acid oxidase is similar

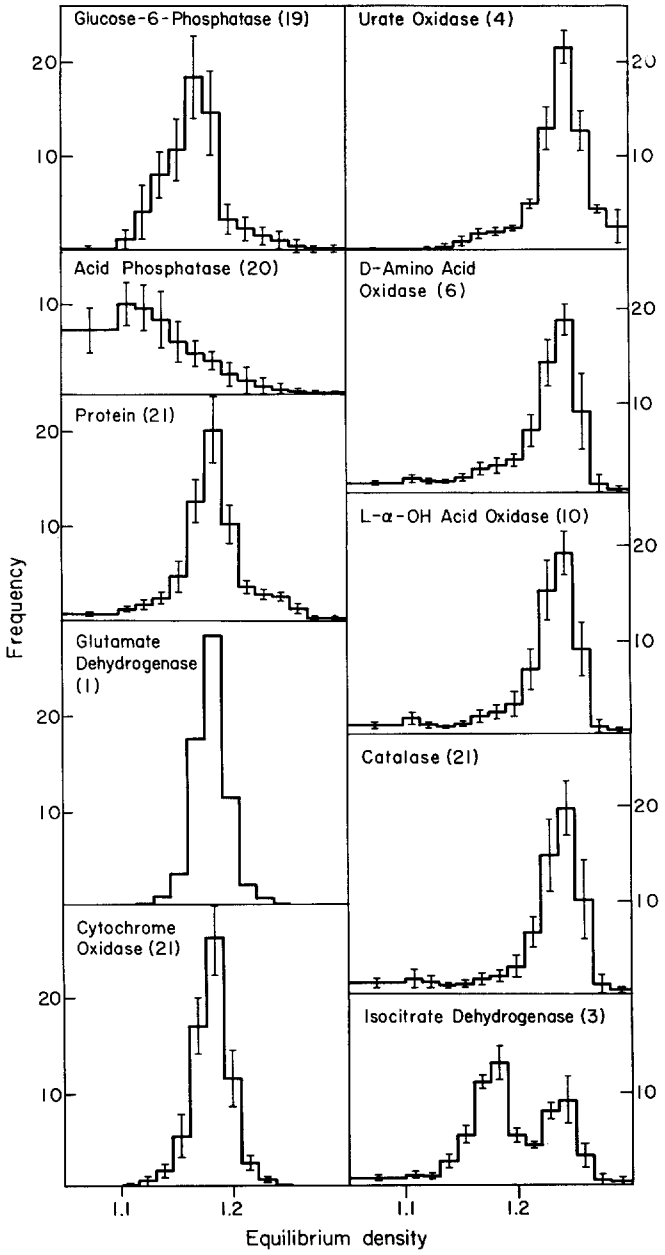

FIGURE 10 Isopycnic subfractionation of λ fraction with automatic rotor. Averaged density frequency distribution histograms. Vertical lines through histogram bars represent standard deviation. Number of experiments is given in parentheses.

to those of catalase and of D-amino acid oxidase. In contrast, urate oxidase occurs in larger amounts in the particulate ν and λ fractions, and shows a corresponding deficit in the ψ fraction. The significance of this difference will be examined below. Table II also presents some results on the distribution of the NADP-linked isocitrate dehydrogenase, which was measured on the fractions after it was found to be a component of peroxisomes in *Tetrahymena pyriformis* (M. Müller and J. F. Hogg, personal communication). Its observed distribution agrees with the results of other workers (22, 29, 42), who have found the greater part of it in the soluble fraction, and the remainder in the mitochondrial fraction. The recovery values listed in Table II, which apply to the over-all fraction-

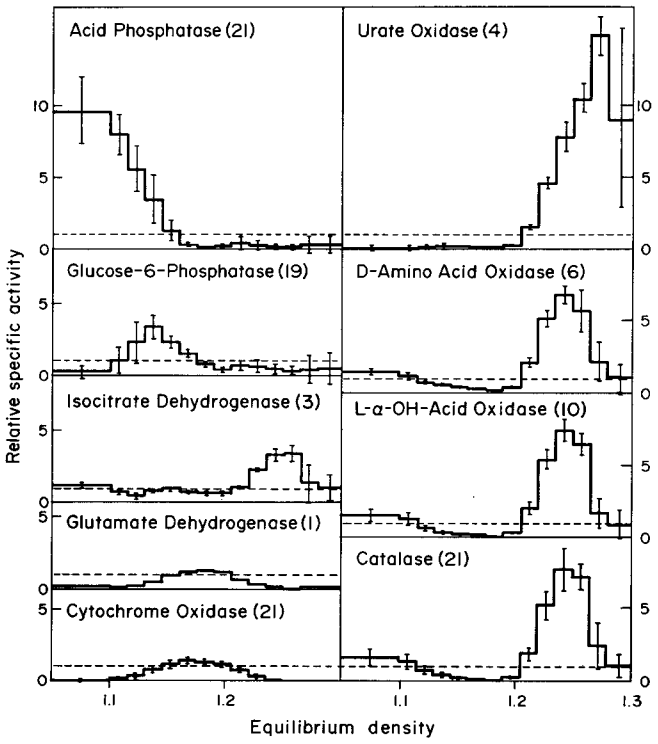

FIGURE 11 Isopycnic subfractionation of λ fraction. Graph shows specific activity of enzymes, expressed in terms of their specific activity in the λ fraction, as a function of density. Data were obtained from the standardized density distribution histograms, as for Fig. 10, and averaged. Vertical lines through histogram bars represent standard deviation. Number of experiments is given in parentheses.

ation, including the density gradient step, are satisfactory for most enzymes except urate oxidase. The 20% loss of urate oxidase recorded here is comparable to that suffered in earlier experiments (4, 21).

The graphs of Figs. 10 and 11, together with the median density values listed in Table III, illustrate the efficiency and reproducibility of the density gradient centrifugation procedure. The mitochondrial enzymes, cytochrome oxidase and glutamate dehydrogenase, equilibrate as a single sharp symmetrical band around a density of 1.18, in contrast with earlier experiments in which median density values of at least 1.19 were observed (11). As mentioned above, the missing shoulder on the dense side accounts for this difference (See Fig. 9). Protein shows a similar, but somewhat flatter distribution pattern, with a significant hump in the peroxisome region. Removal of the peroxisomes, lysosomes, and other contaminants raises the specific activity of cytochrome oxidase by some 35% in the major mitochondrial subfractions (Fig. 11).

The distribution of acid phosphatase around a density of 1.12 is in essential agreement with the results of Wattiaux and coworkers (50, 51). Unfortunately, the treatment of the animals with Triton WR-1339 does not cause an equally drastic decrease in the density of all lysosomes, and these still overlap to some extent with the mitochondria. Very occasionally, we have observed a second small peak of lysosomes at their normal density value of 1.21, indicating that a small proportion of the particles had escaped invasion by the injected detergent. This observation was infrequent enough not to appear in the statistical graph of Fig. 10. As seen in Fig. 11, the highest specific activity of acid phosphatase occurs in the original layer, where the lighter lysosomes remain arrested at the top of the gradient. Soluble enzymes released from injured lysosomes may also be present in this fraction.

The broad distribution of glucose-6-phosphatase around a density of about 1.17 differs from that found in microsomal subfractions separated in the same manner, but with a centrifugation time of 3 hr (J. Berthet and H. Beaufay, personal communication). It reflects incomplete density equilibration of the microsomes under the conditions adopted, which is an advantage since it decreases the microsomal contamination of the peroxisomes.

TABLE III

Median Density of Particulate Enzymes

Values listed are means ± standard deviation.

Enzyme	No. of experiments	Median density
Protein	21	1.181 ± 0.003
Acid phosphatase	21	1.117 ± 0.014
Glucose-6-phosphatase	20	1.167 ± 0.005
Cytochrome oxidase	21	1.179 ± 0.003
Glutamate dehydrogenase	1	1.181
Isocitrate dehydrogenase	3	(1.187 ± 0.006)*
Catalase	21	1.233 ± 0.005
L-α-Hydroxy acid oxidase	10	1.231 ± 0.004
D-Amino acid oxidase	6	1.230 ± 0.004
Urate oxidase	4	1.240 ± 0.002

* Bimodal distribution (see Fig. 10).

The three soluble peroxisomal enzymes, catalase, D-amino acid oxidase, and L-α-hydroxy acid oxidase, show almost identical distribution patterns around a density of 1.23, and are clearly separated from the mitochondria, as indicated by a sevenfold increase in specific activity in the peak fractions. Small amounts of the three enzymes are also found in the top fractions, probably as a result of their release in soluble form from disrupted peroxisomes. In contrast, urate oxidase, which is firmly bound to the crystalloid core of the peroxisomes (3, 32, 43, 48), is entirely absent from the top fractions and somewhat more abundant than the soluble peroxisomal enzymes in the bottom fractions. This difference is reflected in a higher median equilibrium density (Table III), and shows up strikingly in the specific activity patterns (Fig. 11). An excess of urate oxidase over soluble peroxisomal enzymes has been observed before in density gradient pellets and has been attributed to the presence of isolated cores, which equilibrate at a higher density than intact peroxisomes (11). As will be shown below, our morphological examinations entirely bear out this interpretation. Sedimentation of isolated cores may account similarly for at least part of the difference in distribution between urate oxidase and the other peroxisomal enzymes after differential centrifugation (Table II). A unique bimodal distribution was found for isocitrate dehydrogenase, with clearcut peaks coinciding with those of mitochondria and of peroxisomes. Apparently, this enzyme activity is associated with the two types of particles, in addition to being present in the cell sap in much larger amounts.

Biochemical Properties of Purified Fractions and Further Purification

Our main aim in these experiments being a preparative one, we have selected and pooled for further study those subfractions which, on the basis of biochemical analysis, allowed a satisfactory yield without excessive loss of purity. The top layers down to a density of about 1.13 provided the lysosomal fraction, cuts between about 1.16 and 1.20 gave the mitochondrial fraction, and the layers below 1.22 formed the peroxisomal fraction. The main biochemical properties of the pooled fractions are listed in Table IV. The yields in purified particles, as estimated by their specific reference enzymes, vary between 10 and 20% of the total liver content, and correspond for each type of particle to about half the amount recovered in the λ fraction. Lysosomes are purified almost 20-fold, mitochondria 4.25-fold, and peroxisomes about 35-fold, over the original homogenate. The discrepancy between urate oxidase and the soluble peroxisomal enzymes comes out clearly: urate oxidase is purified 50-fold in the peroxisomal fraction, but is absent from the lysosomal fraction in which the soluble enzymes are purified sixfold. Mitochondria, which are almost absent from the peroxisomal fraction, are present in nonnegligible amounts in the lysosomal fraction.

In a number of experiments, the lysosomes were further purified by Trouet's flotation procedure as described under Materials and Methods. As shown in Table V, this procedure yielded lysosomes practically devoid of mitochondrial, peroxisomal, and microsomal marker enzymes. The preparations were of distinctly lower purity when the procedure was applied directly to an M + L fraction. However, this may be caused simply by a less thorough removal of the fluffy layer in the isolation of this fraction, since microsomes are the main contaminant.

Despite numerous attempts, we were unable to increase the purity of the peroxisomal fraction. We tried differential sedimentation, flotation through a continuous density gradient from a

TABLE IV

Properties of Purified Fractions from Isopycnic Density Gradient Centrifugation

Values listed are means ± standard deviation.

Enzyme	No. of experiments	Composition of purified fractions (% of content of whole liver)			Relative specific activity (with respect to whole liver)		
		Lysosomal fraction	Mitochondrial fraction	Peroxisomal fraction	Lysosomal fraction	Mitochondrial fraction	Peroxisomal fraction
Protein	21	0.65 ± 0.22	4.3 ± 0.8	0.47 ± 0.1	1.00	1.00	1.00
Acid phosphatase	21	11.4 ± 2.4	2.1 ± 0.9	0.13 ± 0.2	18.9 ± 5.7	0.49 ± 0.2	0.27 ± 0.4
Glucose-6-phosphatase	19	0.24 ± 0.3	0.96 ± 0.5	0.04 ± 0.05	0.31 ± 0.3	0.22 ± 0.1	0.09 ± 0.08
Cytochrome oxidase	21	0.58 ± 0.7	18.1 ± 4.2	0.05 ± 0.06	0.87 ± 1.3	4.25 ± 0.9	0.11 ± 0.1
Glutamate dehydrogenase	1	0.94	24.1	0.15	1.19	4.48	0.25
Isocitrate dehydrogenase	3	0.43 ± 0.04	2.4 ± 0.3	1.06 ± 0.18	0.76 ± 0.41	0.61 ± 0.11	2.57 ± 0.57
Catalase	21	3.5 ± 1.1	2.6 ± 1.9	17.1 ± 4.9	5.8 ± 2.5	0.60 ± 0.4	36.3 ± 6.4
L-α-Hydroxy acid oxidase	10	3.1 ± 1.0	2.9 ± 1.3	15.9 ± 4.7	5.7 ± 2.3	0.71 ± 0.3	35.8 ± 7.2
D-Amino acid oxidase	6	2.5 ± 0.5	3.2 ± 1.3	12.4 ± 4.6	5.8 ± 1.9	0.81 ± 0.3	30.0 ± 7.7
Urate oxidase	4	0.15 ± 0.3	2.9 ± 1.1	18.4 ± 4.3	0.43 ± 0.9	0.81 ± 0.2	50.0 ± 14.4
Total yield (mg proteins from 100 g liver)					170	1100	120

TABLE V

Purification of Lysosomes by Flotation Method of Trouet (47)

Values given are means ± standard deviation.

Starting material / Enzyme	M + L fraction					Lysosomal fraction from gradient				
	No. of exp.	Yield (% of liver)		Relative specific activity		No. of exp.	Yield (% of liver)		Relative specific activity	
		Lysosomes	Residue*	Lysosomes	Residue*		Lysosomes	Residue*	Lysosomes	Residue*
Protein	17	0.54 ± 0.29	20.2 ± 1.1	1.00	1.00	9	0.18 ± 0.06	1.1 ± 0.45	1.00	1.00
Acid phosphatase	17	19.7 ± 6.0	16.1 ± 7.5	39.1 ± 9.3	0.79 ± 0.34	8	8.23 ± 1.7	5.1 ± 1.2	48.5 ± 13.9	5.6 ± 2.0
Glucose-6-phosphatase	10	0.37 ± 0.42	7.1 ± 3.3	0.85 ± 1.0	0.35 ± 0.16	2	0	0.77 ± 0.07	0	0.66 ± 0.01
Cytochrome oxidase	12	0.08 ± 0.08	69.0 ± 14.6	0.17 ± 0.14	3.42 ± 0.75	4	0.02 ± 0.01	3.59 ± 1.8	0.07 ± 0.03	2.39 ± 0.67
Catalase	17	0.02 ± 0.03	48.4 ± 9.7	0.05 ± 0.08	2.41 ± 0.55	5	0.02 ± 0.02	4.28 ± 1.4	0.09 ± 0.07	4.27 ± 0.76

* Remaining in initial bottom layer (see Fig. 2). Two intermediate layers contained very little protein and enzymatic activities.

TABLE VI

Composition of Fractions

For method of calculation, see text. The enzymic data used for the computations are taken from Tables II for the λ fraction, V for the T and G-T lysosomal fractions, and IV for the others.

Preparation	Percentage of total protein of preparation contributed by				
	Endoplasmic reticulum	Lysosomes	Mitochondria	Peroxisomes	Other components
Liver	21.5 (*e*)	2.03 (*l*)	20.2 (*m*)	2.53 (*p*)	53.7
λ Fraction	6.4	4.7	64.6	12.3	12.0
Lysosomal fraction*					
G-T	0	98.4	1.4	0.2	0
T	18.3	78.2	3.4	0.1	0
G	6.7	37.8	17.6	13.3	24.6
Mitochondrial fraction	4.7	1.0	85.8	1.5	7.0
Peroxisomal fraction	1.9	0.5	2.2	95.2	0.2

* G = isolated by continuous gradient procedure; T = isolated by flotation method of Trouet (47); G-T = isolated by the two procedures in succession.

bottom layer made up to a density of 1.28 with additional sucrose, and zonal electrophoresis in a sucrose gradient containing 25 mM imidazole-HCl buffer pH 7. Except for the removal of excess urate oxidase, which remained in the bottom layer in the flotation experiment as would be expected for the denser cores, all these procedures failed to increase the purity of the preparation, as assessed by the specific activity of catalase. Analysis of the peroxisomal fraction by the boundary method of density gradient differential centrifugation (10, 23) also indicated a high degree of homogeneity of all the subfractions.

Quantitative Evaluation of the Protein Content of Subcellular Components

We have attempted to evaluate the contribution of each subcellular component to the total protein content of the isolated fractions by introducing the basic assumption that marker enzymes have the same specific activity in all subgroups of their host-particles separated by the fractionation procedure (postulate of biochemical homogeneity). Then we may write, for any preparation:

$$100 = eG + lA + mO + p\,(0.9C + 0.1U) + X \quad (1)$$

in which e, l, m, and p are the percentages of total liver protein constituted by endoplasmic reticulum, lysosomes, mitochondria, and peroxisomes, respectively.

G, A, O, C, and U are the relative specific activities of glucose-6-phosphatase, acid phosphatase, cytochrome oxidase, catalase, and urate oxidase, respectively.

X is a term, designated percentage of unassigned protein, which includes any additional component that may be present in the preparation, as well as discrepancies resulting from analytical errors (or from the lack of validity of the underlying postulate of biochemical homogeneity).

The peroxisome term of equation (*1*) is broken down into two components representing the soluble proteins and the crystalloid core, which constitute approximately 90 and 10% of the total particle proteins, respectively.[2] We thereby account for the differences in distribution between urate oxidase and the soluble peroxisomal enzymes due to particle disruption. The correction involved is a minor one, except for the bottom gradient fractions in which urate oxidase is in considerable excess.

We tested equation (*1*) by applying the mathematical technique of linear programming (26) to

[2] F. Leighton, B. Poole, and C. de Duve. To be published.

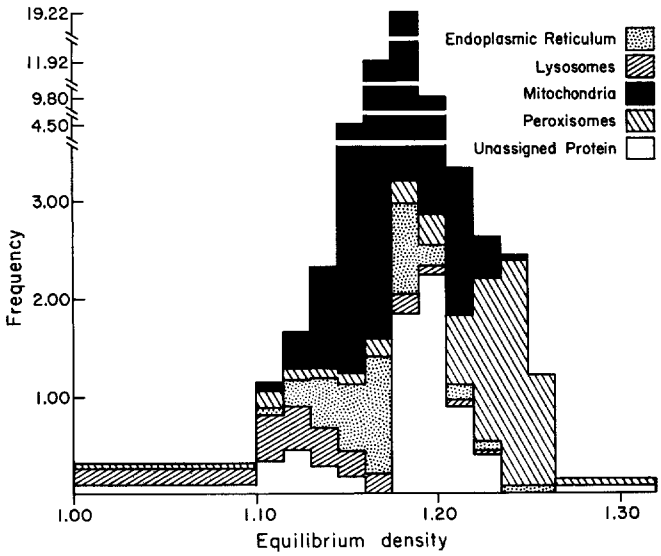

FIGURE 12 Computed contribution of each subcellular component to the total protein content of the fractions isolated by isopycnic density gradient centrifugation. For method of calculation, see text.

the enzymic data obtained on the gradient subfractions, searching for a combination of coefficients that would minimize the total amount of unassigned protein, and hence provide upper limits for the coefficients themselves. In order to arrive at acceptable results, we had to include in the program information provided by other fractions. The value of l was set at 2.03, the maximum compatible with the data obtained on the purest lysosomal fraction G-T (Table VI). In turn, the coefficient e was evaluated at 21.5 from the maximum amount of protein attributable to glucose-6-phosphatase in the T fraction, after lysosomes, mitochondria, and peroxisomes had been accounted for (Table VI).

The results of this computation are shown graphically in Fig. 12 for the gradient subfractions, and numerically in Table VI for the main purified fractions. Virtually no unassigned protein is attributed to the purest lysosome and peroxisome fractions, a fact which indicates, in agreement with the premises of the calculation, that our estimates of the coefficients l and p are upper limits. Their true values could, of course, be lower, in which case the fractions would contain more unassigned protein than estimated, and their purity would be correspondingly lower. The biochemical evidence does not disprove this possibility, since it indicates only that further purification could not be achieved with the methods tried. However, as will be shown below, the morphological results do demonstrate that the biochemical evaluation of the purity of our fractions is, in fact, a correct one. As to the values of e and m, they are obviously of the right order of magnitude in view of all the evidence indicating that both the mitochondria and the microsomal membranes each account for about 20% of the total liver protein.

Fig. 12 shows that, except for a small peak associated with the top fractions and probably representing soluble proteins incompletely removed by washing from the λ fraction, the major part of the unassigned protein occurs as a sharp band included with the denser mitochondria around a density of 1.20. If we bar a systematic error in the measurements, this band reflects either the presence of an additional component for which no biochemical marker has been foreseen, or a lack of biochemical homogeneity of the mitochondria. This question will be discussed below in the light of the morphological observations.

Mitochondrial Localization of Cytoplasmic DNA

The recent interest in mitochondrial DNA prompted us to investigate with our method the precise distribution of particle-bound cytoplasmic DNA in rat liver, since the current belief that this DNA is localized in mitochondria, and not in other cytoplasmic particles, rests almost exclusively on morphological arguments. Lacking a chemical

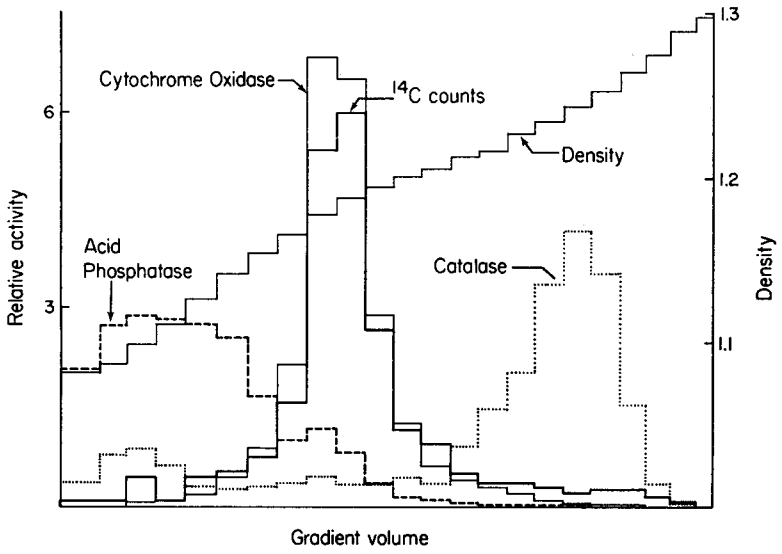

FIGURE 13 Isopycnic subfractionation of M + L fraction from rat injected 4 days previously with Triton WR-1339 and with 10 μc thymidine-^{14}C (25 μc/mmole). Aliquots of gradient fractions were dried, dissolved in hyamine hydroxide, and counted in a scintillation counter with external standardization. For definition of ordinate, see Fig. 9.

method sufficiently sensitive to be applicable to the small amounts of DNA present in gradient subfractions, we resorted to in-vivo labeling with thymidine-^{14}C as an indirect means of assaying DNA. A number of experiments were done on both M + L and λ fractions, at various times after injection of the labeled thymidine. In all cases, the distribution of ^{14}C counts paralleled closely that of cytochrome oxidase, and little or no radioactivity was found in the lysosome or peroxisome regions. The results of one such experiment are shown in Fig. 13. Thus, if the radioactivity does, indeed, belong to DNA, these findings demonstrate that the metabolically mobile DNA of mitochondrial fractions is present in the true mitochondria.

Morphological Properties of Purified Fractions

By scaling up our separation techniques, we have been able for the first time to separate "visible" quantities of the rarer lysosomes and peroxisomes. The color photograph of the three peak fractions shown in Fig. 14 gives an idea of the macroscopic appearance of such suspensions. When filled with the colorless Triton WR-1339, as they are in these experiments, the lysosomes appear deep orange. They are likely to be a darker brown in normal liver. On the other hand, the peroxisomes have a greenish tinge which they undoubtedly owe to their richness in catalase. The pink color of the purified mitochondria presumably reflects their high content in cytochromes, and contrasts with the light tan color of mitochondrial fractions isolated in the usual way.

Some selected fractions from a regular density gradient run were examined in the electron microscope. Their biochemical composition, as estimated from their enzyme content by means of equation (*1*), is shown in Table VII. As indicated by the values between parentheses, it is likely that, for the animals used in this particular experiment, the mitochondrial coefficient is somewhat lower and the peroxisomal coefficient somewhat higher than the statistically estimated values given in Table VI. Whether we use the statistical coefficients or revise them to minimize the amount of unassigned protein of the fractions, the results of the calculation remain essentially in agreement with the data of Table VI and of Fig. 12. In particular, the largest proportion of unassigned protein is found in fraction 14, which has a density of 1.21 (compare with graph of Fig. 12).

Electron micrographs of these fractions and of a highly purified preparation of lysosomes filled with Triton WR-1339 are shown in Figs. 15–18. In Table VIII are listed the results of the measure-

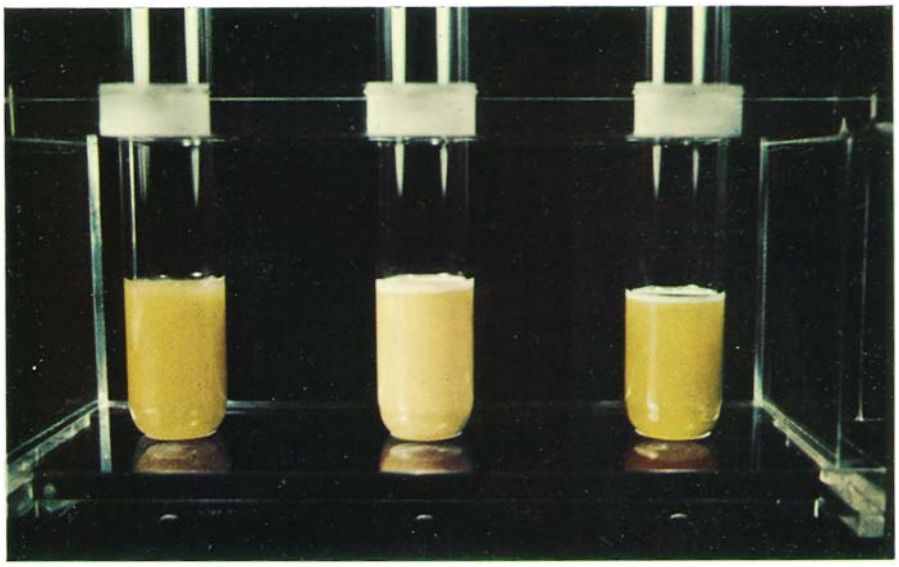

FIGURE 14 Isopycnic subfractionation of λ fraction. Photograph of tubes containing highest specific activity of acid phosphatase (left), cytochrome oxidase (middle), and catalase and oxidases (right). Magnification, normal size. Photograph taken by Dr. J. T. Finkenstaedt.

ments made on the micrographs. The criteria of identification of the structures mentioned in this Table were as follows:

The "condensed form" of mitochondria is that seen most frequently in the micrographs of Fig. 15. It is characterized by a shrunken and condensed matrix, with a corresponding dilatation of the space between the inner and outer membranes. Clearly derived from this form are the "dense fragments," which appear as matrices or fragments thereof, showing the same density as in the condensed form, but freed from the outer envelope (Figs. 15 *a* and 16). The term "swollen form" has been given to the images seen with the greatest frequency in Fig. 16 (see also Fig. 15 *a*). Some resemble normal mitochondria in situ, but many show evidence of excessive swelling, with disruption of the outer membrane.

Peroxisomes (microbodies) were recognized by their sharply etched single outer membrane, uniform matrix of moderate opacity, and inner core, when included in the section. The fine structure of the peroxisome core was rarely visible and this made the identification of free cores somewhat difficult. However, these could generally be recognized and distinguished from dense mitochondrial fragments by their ragged edges (Fig. 17 *b*). They were detected less easily in Fig. 17 *a* owing to the close packing of the particles.

Only membranous structures studded with ribosomes were designated endoplasmic reticulum. All the profiles attributed to lysosomes had the appearance of normal pericanalicular dense bodies, with no evidence of stored Triton WR-1339 (see Figs. 16 and 17 *a*). As shown in Fig. 18, the swollen Triton-filled lysosomes seemed to resist fixation very poorly. Many appear disrupted, with consequent curling of their membranes into whorls and release of their contents, which presumably form the amorphous material seen packed against the filter.

Direct comparison between the morphological and biochemical data is provided by the graphs of Fig. 19. On the whole, the agreement between the two types of estimates is surprisingly good, and establishes the validity of the figures given in Table VI for the purity of our best fractions and for the proportion of the total hepatic protein associated with lysosomes and peroxisomes in our animals. Furthermore, the morphological analysis of fraction 14 provides a likely identification of the band of unassigned protein detected around a density of 1.20 by the method of linear programming (Fig. 12). We did not see an additional well defined structural component in this fraction,

TABLE VII

Biochemical Properties of Fractions Examined in Electron Microscope

Fractions isolated by standard procedure.

Fraction	Average density	Percentage of total liver protein	Percentage of total protein of preparation contributed by*				
			Endoplasmic reticulum	Lysosomes	Mitochondria‡	Peroxisomes‡	Other components‡
λ	—	7.300	5.5	4.8	67.1(62.0)	12.0(13.9)	10.6(13.8)
2	1.092	0.126	12.3	38.7	13.2(12.2)	19.2(22.3)	16.6(14.5)
9	1.180	1.340	3.4	0.8	103.0(95.1)	0.6 (0.7)	−7.8 (0)
14	1.211	0.139	1.9	3.8	42.4(39.2)	22.5(26.1)	29.4(29.0)
20	1.249	0.092	1.9	1.9	5.3 (4.9)	78.8(91.3)	12.1 (0)
21	1.257	0.033	0	4.9	1.5 (1.4)	70.7(82.0)	22.9(11.7)

* Values calculated by means of equation (*1*) with coefficients given in Table VI. The experimental enzymic data can be obtained in per cent of liver content by dividing values listed by appropriate coefficient and multiplying by protein content (third column).

‡ Values between parentheses are obtained by making $m = 18.65$ and $p = 2.93$.

but rather found it to contain a much larger proportion of swollen mitochondria, of dense fragments of mitochondrial matrices, and of unidentifiable debris, presumably of mitochondrial origin, than fraction 9. It is probable that one or more of these forms have a lower specific cytochrome oxidase activity than the "condensed form" which is predominant in fraction 9, and, in view of the morphological evidence, that preparative damage is responsible for this difference. This interpretation is compatible with the known fragility of cytochrome oxidase and with the tendency of this enzyme to give a somewhat low recovery (Table II).

It has been pointed out above that the new rotor gives a cleaner and more symmetrical mitochondrial band than the SW-39 rotor (see Fig. 9). It now appears from the more refined measurements that have just been discussed that this band is itself not entirely homogeneous, but includes a small subcomponent comprising apparently damaged particles with decreased cytochrome oxidase activity and displaced by about 0.02 density units on the dense side of the main component. This raises the possibility that further mitochondrial damage and displacement may occur in the course of the longer centrifugation in the SW-39 rotor, leading to the appearance of the second cytochrome oxidase band found around a density of 1.22 when this rotor is used (Fig. 9). We have not yet examined this second peak in the electron microscope, but we know that it is associated with significant amounts of unassigned protein, as required by our hypothesis. In nine experiments carried out in swinging bucket rotors, the specific cytochrome oxidase activity was 27% lower in the fractions with an average density of 1.207 than in the fractions with an average density of 1.183. This difference, which is highly significant statistically, could hardly be accounted for by the increased peroxisome content of the denser fractions.

DISCUSSION

Technical Comments

The continuous gradient technique described in this paper is particularly valuable for the purification of peroxisomes and is now being used regularly for further biochemical study of these particles. As isolated, the preparations appear to be in a satisfactory state of structural preservation and to contain only about 5% of biochemically and morphologically detectable contaminants. They are obtained in yields averaging 100 mg of protein per run, with a minimum expenditure of time and effort, 5–6 hr on the part of two investigators. As already pointed out, these gains are to be attributed largely to the use of the new rotor. The advantages of this machine have been discussed in detail elsewhere by Beaufay (8), who has pointed out that it is well suited for many other applications of both analytical and preparative density gradient centrifugation, and that it lends itself to a number of relatively simple

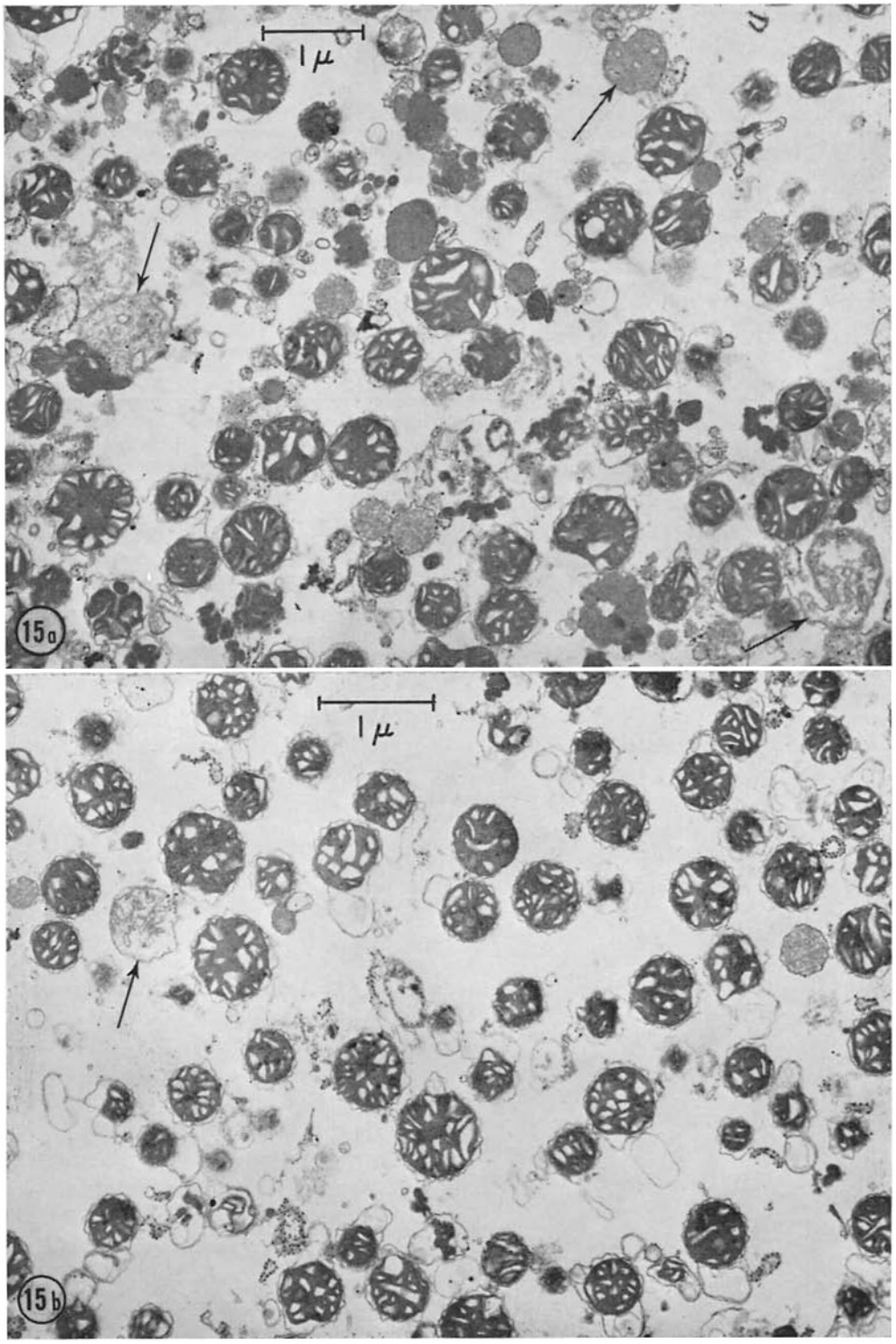

FIGURE 15 Sections through λ fraction and purified mitochondrial fraction 9. *a*, λ fraction. Most mitochondria are in condensed state, but a few are in swollen, partly damaged condition (arrows). Preparation contains, in addition, fairly numerous peroxisomes, a few strands of rough endoplasmic reticulum, and a background of amorphous and membranous material, some of which is probably of lysosomal origin. × 15,000. *b*, Fraction 9. Almost all mitochondria are in condensed state. One swollen mitochondrion is seen in field (arrow). Contaminants are much rarer than in λ fraction. × 17,000.

TABLE VIII

Morphological Properties of Fractions

Fractions are those described in Table VII and illustrated in Figs. 15–17.

Constituent	Percentage of total particulate volume			
	Fraction 9	Fraction 14	Fraction 20	Fraction 21
Endoplasmic reticulum	3.5	2.5	0.7	1.9
Lysosomes	~0.2	3.6	3.0	5.5
Mitochondria				
Condensed form	81.0	22.1		
Dense fragments	3.3	11.8	0	2.5
Swollen form	5.0	23.3		
Peroxisomes				
Intact	0.6	24.5	93.8	73.1
Isolated cores			1.0	9.6
Unidentified	6.4	12.2	1.5	7.4

modifications designed to improve even further the capacity or the separation efficiency or both.

The technique is less suitable for the preparation of lysosomes, which are obtained in a state of relatively low purity and can be purified more easily and in greater quantities by the procedure of Trouet (47). However, the partly purified lysosomal fractions obtained by the continuous gradient procedure provide a convenient starting material for further purification and have yielded particularly pure preparations of lysosomes (Table V).

Another interesting byproduct of the separation is represented by mitochondria, which are obtained largely free of both lysosomes and peroxisomes. We do not yet know to what extent mitochondria prepared in this manner maintain their functional integrity. In any case, it seems unlikely that such a cumbersome procedure will replace current separation methods in the usual studies of mitochondrial function. But it may be very valuable, especially if modified to give a greater yield of mitochondria, when one wishes to check the possible part played by lysosomes or peroxisomes in the phenomena observed on cruder fractions, or to verify the precise localization of some trace component. An example of such an application is given by the experiment in which we have verified the mitochondrial localization of the metabolically active DNA present in mitochondrial fractions.

One main drawback of the method is that it requires a preliminary treatment of the animals with Triton WR-1339. This is particularly unfortunate in the case of the lysosomes, since these particles are definitely abnormal as isolated, and contain large amounts of Triton WR-1339 (50, 51) and several plasma proteins (47). There is no sign that mitochondria or peroxisomes are affected by the treatment, but this is by no means unlikely, since Triton WR-1339 is known to cause dramatic changes in lipid and cholesterol metabolism (13, 25, 39, 49). Unfortunately, a separation system allowing a satisfactory resolution of mitochondria, lysosomes, and peroxisomes from normal liver has not yet been found.

Although not essential to the success of the operation, the various automated analytical procedures used in our work amply repaid the time and effort invested in setting them up. While being at least as accurate and reproducible as their manual counterparts, they are distinctly faster and less exposed to chance errors. Requiring a minimum of attention, they are called upon much more freely, and have, in the present case, allowed a much more rigorous and complete control of the quality of each preparation than would have been possible with the usual methods. They have been invaluable in the further biochemical analyses of the purified particles, to be reported in subsequent papers.

Two new methods of evaluating the composition

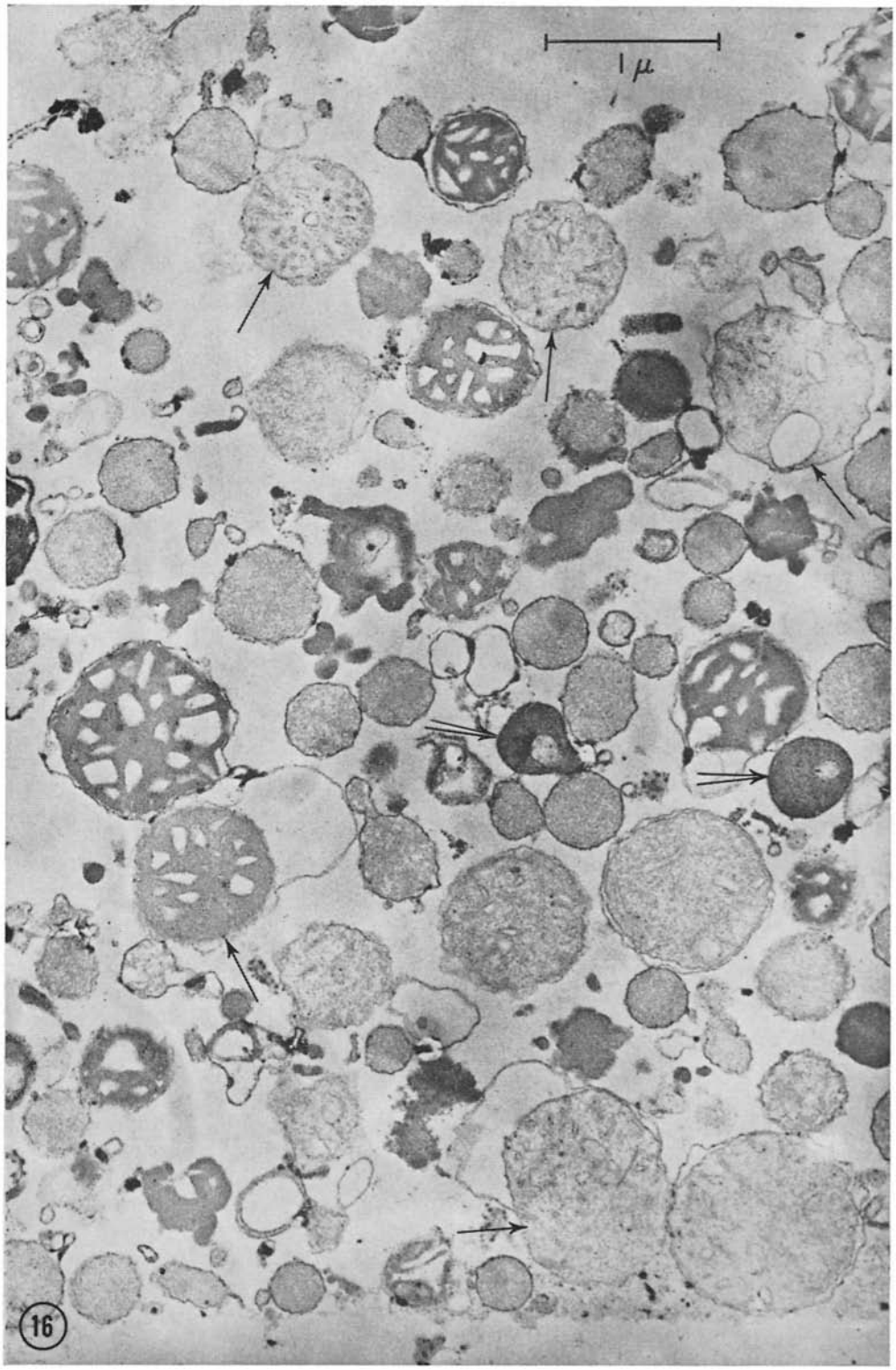

FIGURE 16 Section through fraction 14. Most mitochondria are in swollen, partly damaged state. Many have partly or entirely lost outer membrane (arrows). Field also includes many peroxisomes, various debris probably mostly of mitochondrial origin, a little rough endoplasmic reticulum, and two lysosomes of normal appearance (double arrows). × 25,000.

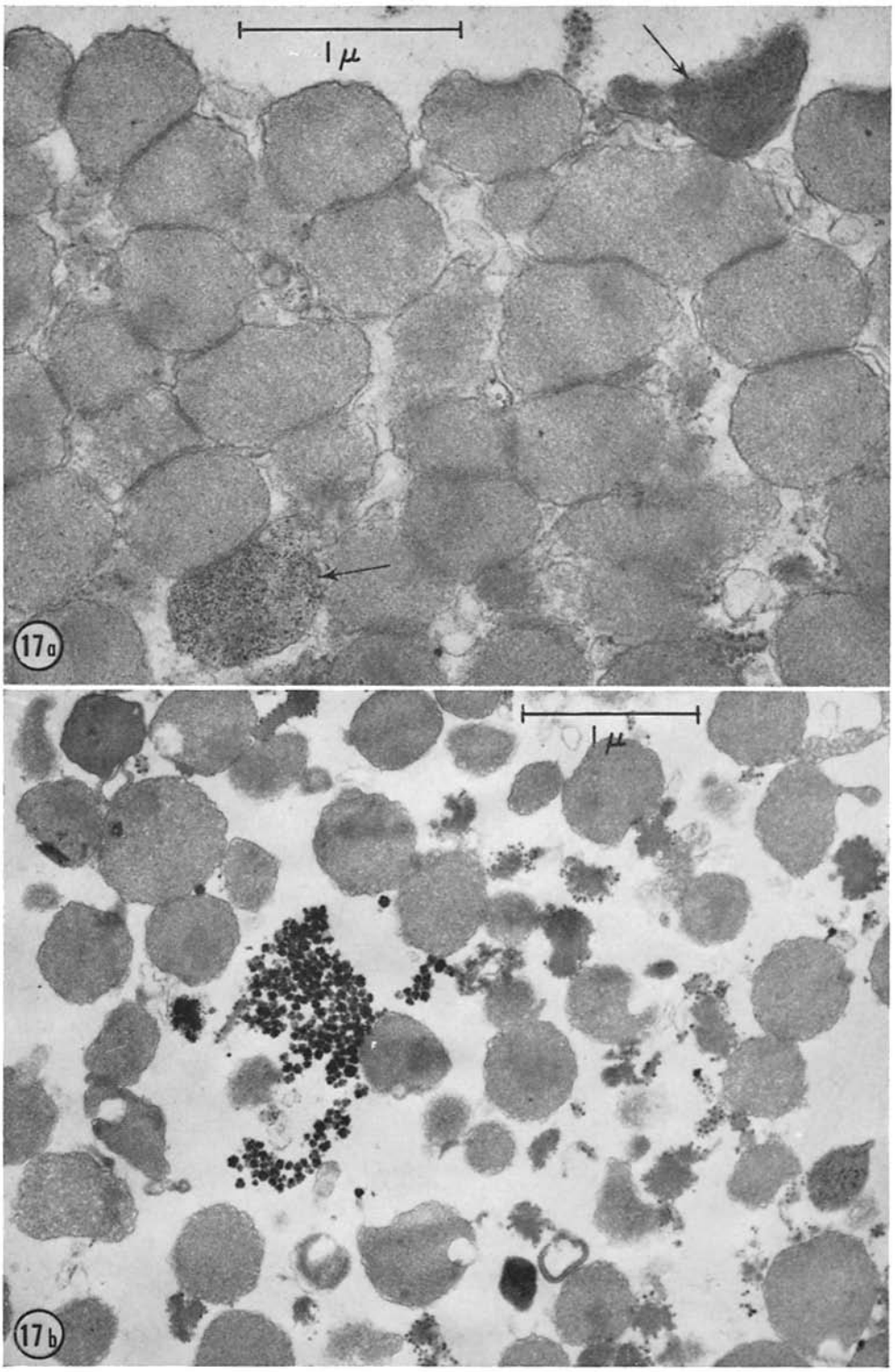

FIGURE 17 Sections through peroxisome-rich fractions 20 and 21. *a*, Fraction 20. Peroxisomes fill the field. Their appearance is normal, except that the core does not show up very distinctly. Two lysosomes that have not taken up any Triton WR-1339 (arrows), and two small strands of rough endoplasmic reticulum are the only contaminants. × 32,000. *b*, Fraction 21. Peroxisomes are, by far, the main component, but contaminants and isolated cores are more conspicuous than in fraction 20. Clusters of dense granules are glycogen particles. × 26,000.

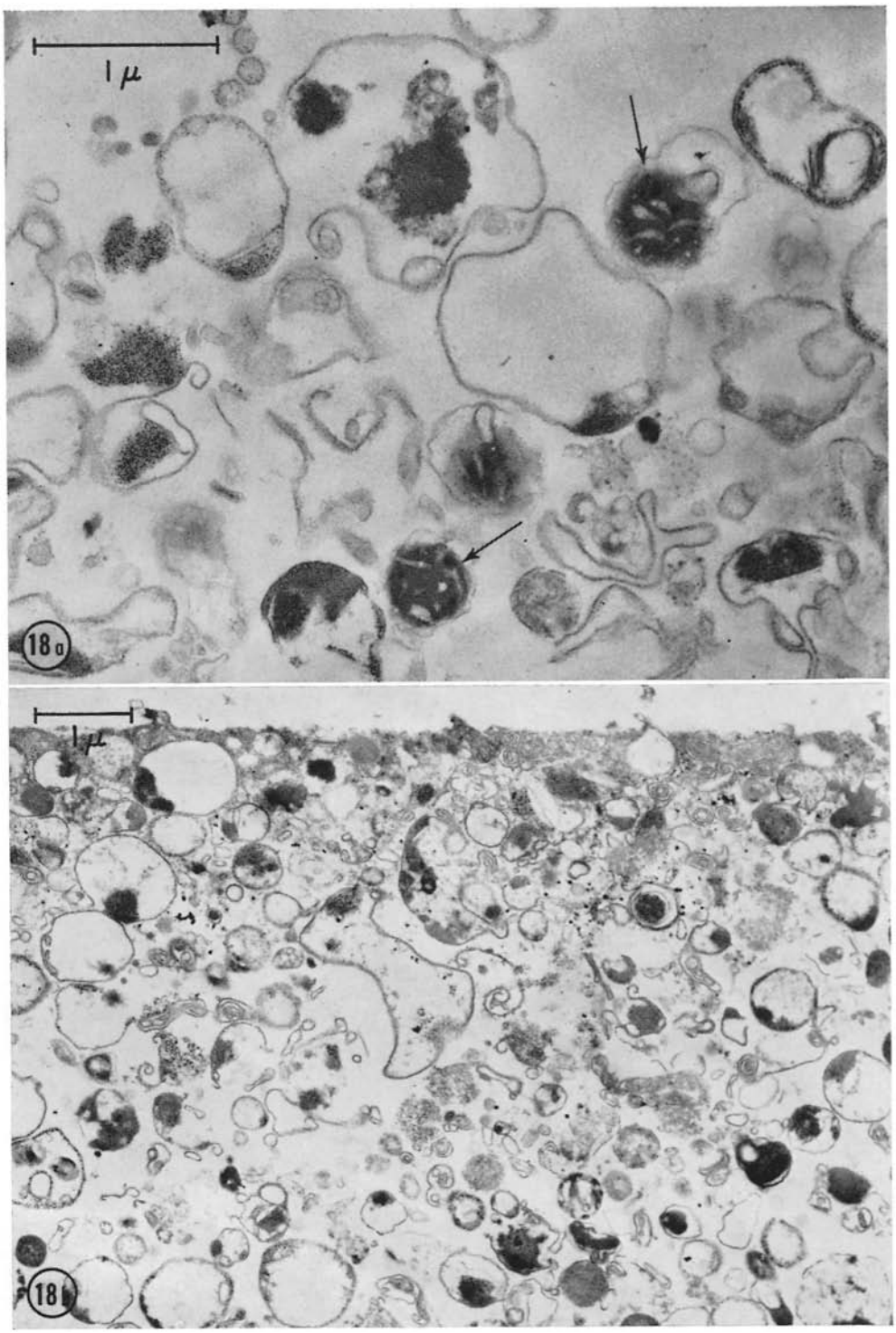

FIGURE 18 Sections through lysosome-rich fraction 2 and through a GT fraction subjected to further purification by procedure of Trouet (47). *a*, Fraction 2. Remnants of original lysosomal matrix, dotted with ferritin-like particles, are seen within swollen lysosomes filled with Triton WR-1339. Several particles have ruptured curled-up membrane, presumably as a result of damage sustained during or after fixation. Two mitochondria (arrows) and some rough endoplasmic reticulum are present. × 27,000. *b*, Purified GT fraction. Intact lysosomes have same structure as in fraction 2. Fraction also contains many small vesicles, as well as numerous curled-up membranes and a considerable amount of amorphous material, presumably originating from damaged lysosomes. Mitochondria cannot be detected. × 14,000.

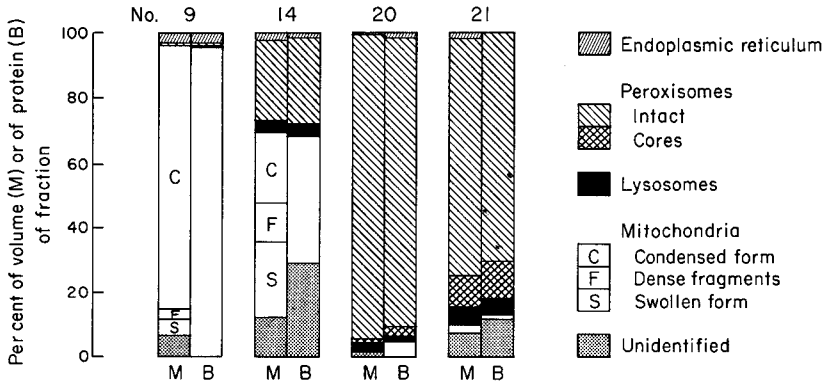

FIGURE 19 Composition of fractions as assessed by morphological (*M*, see Table VIII) and biochemical (*B*, see Table VII, figures in parentheses) methods. Free cores were estimated biochemically by assigning the coefficient 0.293 (10% of the protein of intact peroxisomes) to the excess of urate oxidase over catalase activity (see equation *1*).

and purity of the fractions have been introduced in this work. One, morphological, applies standard morphometric techniques to representative micrographs. It owes its quantitative value mainly to the use of the Millipore filtration method of Baudhuin et al. (6) which allows true random sampling of the fractions. The other, biochemical, rests on less secure premises, combining the assumption of biochemical homogeneity with the additional condition that the total amount of unassigned protein be minimized. Thus, the computation procedure is designed to provide the most favorable evaluation of purity of the fractions compatible with the postulate of biochemical homogeneity. In the present application, the two methods have yielded surprisingly concordant results, with only one serious discrepancy which turned out to be informative rather than invalidating. This agreement by no means establishes the general validity of our calculation method, but it provides support both for its underlying assumptions and for the quantitative results, as related to this particular set of data.

Properties of Particles

Our enzymic results largely confirm earlier findings, but some new facts have come to light. The association of L-α-hydroxy acid oxidase with the peroxisomes, referred to briefly in earlier publications (7, 18), is clearly established. Both in the fractionation of whole liver (Table II) and in the subfractionation of the λ fraction (Tables III and IV, Figs. 10 and 11), the enzyme behaves almost identically like catalase and D-amino acid oxidase. An original and surprising observation relates to the distribution of the NADP-linked isocitrate dehydrogenase. As first shown by Hogeboom and Schneider (29) on mouse liver and confirmed later on rabbit (42) and rat (22) liver, some 10–20% of this activity sediments with the mitochondrial fraction, the remainder being in the final supernatant. In *Tetrahymena pyriformis*, about one-half of the activity is soluble and most of the other half is associated with peroxisomes; the mitochondria contain small but significant amounts of this enzyme (M. Müller and J. F. Hogg, personal communication). Our results indicate that in rat liver, the enzyme similarly occurs both in the mitochondria and in the peroxisomes, in addition to being present in large amounts in the cell sap. This is a unique distribution which requires further study.

Attention has already been drawn to the remarkable similarity in distribution between the three soluble peroxisomal enzymes, catalase, D-amino acid oxidase, and L-α-hydroxy acid oxidase. Furthermore, evidence has been presented (see particularly Fig. 19) indicating that the differences in distribution between urate oxidase and the soluble enzymes are entirely explicable by the fact that urate oxidase, when not associated with peroxisomes, does not occur in truly soluble form as the other enzymes do, but remains associated with the sedimentable core. The conclusion emerging from these results is that intact peroxisomes contain all four enzymes essentially in the proportion in which they are present in whole liver, and consequently that the amounts

of the soluble enzymes present in free form in the homogenate are made up by a corresponding amount of free cores. This conclusion strengthens the contention made in an earlier paper (11) that all four enzymes are entirely associated with peroxisomes in the intact cells and that the peroxisomes are biochemically homogeneous. However, its validity remains limited by the accuracy of our enzyme assays, and especially by the extent of our final recoveries. These are fairly satisfactory for the soluble enzymes, but unfortunately they are distinctly deficient for urate oxidase. One must also allow for the possibility, so far unsupported by any morphological observation, that the contents of peroxisomes, including their cores, may occur in free form in the cytoplasm.

According to the evaluation arrived at by linear programming (Table VI), which is directly supported by our morphological measurements (Fig. 19), the whole peroxisome population in the livers of our animals contains about 2.5% of the total liver protein, or 6.5 mg of protein per g wet liver. This is twice the estimate given by de Duve and Baudhuin (18), which, however, was derived in a very indirect fashion. More directly comparable are the measurements made on tissue sections by Loud et al. (35), who state that microbodies occupy 0.77% of the cytoplasmic volume of parenchymal cells, which corresponds roughly to 6 mm^3 per g wet liver (see reference 5). This is one-fourth the minimum volume necessary to accommodate 6.5 mg of protein within particles having a density of 1.10 and a water content of 75% (17). As already mentioned, our estimate of the protein content of the peroxisomes rests on convincing biochemical and morphological evidence; we can reduce it only, and then by no more than about 30%, by assuming that the peroxisomal enzyme activities that are found free in the homogenate do not, as we believe, originate from injured peroxisomes, but occur as such in the intact cells. Even so, our irreducible minimum value of the total peroxisomal volume would still be almost three times that given by Loud et al. (35). The latter value could be underestimated somewhat through lack of recognition of all the particle profiles in the sections, but hardly by a factor of 200%. We can only conclude either that the dimension of peroxisomes is selectively decreased relative to that of other cytoplasmic components as a result of fixation and embedding, or that our animals have more or bigger hepatic peroxisomes than those examined by Loud et al. (35), possibly as a consequence of the treatment with Triton WR-1339. It may be recalled in this connection that treatment of animals with some drugs, such as ethyl chlorophenoxyisobutyrate, causes a considerable increase in the number of peroxisomes in the liver (28, 45). Further work will have to be done to settle this question.

Our estimate of the protein content of the lysosomes, which has been evaluated at 2.0% of the total protein content of the liver (Table VI), is likewise higher than the maximal value of 1.4 which can be derived from the results of Sawant et al. (38), who have isolated lysosome preparations in which several enzymes were purified about 70-fold over the homogenate. However, this difference is easily explained as a consequence of the injection of Triton WR-1339, which causes a considerable increase in the size of the lysosomes (50, 51). It is also possible that our preparations contain enzymically inactive phagosomes or pinocytic vacuoles, in addition to true lysosomes.

As far as the mitochondria are concerned, our calculations have suggested that structural damage, rather than an intrinsic biochemical heterogeneity, may be responsible for the differences in specific cytochrome oxidase activity observed between separate mitochondrial subfractions. This point may be relevant to the evidence of enzymic heterogeneity of mitochondrial subfractions recently reported by Swick et al. (46). The appearance of the mitochondria in our fractions is itself of interest. As shown by Fig. 15, there is no visible difference between mitochondria maintained in 0.25 M sucrose (λ fraction) and those exposed to a seven-fold increase in osmotic pressure (fraction 9). Both are in condensed form, suggestive of a considerable dehydration of the matrix, presumably owing to osmotic imbalance. Such a feature is understandable in fraction 9, but surprising in the isotonic λ fraction. As shown by Hackenbrock (27), mitochondria assume a condensed form when kept anaerobically, and regain their normal shape upon aerobic incubation under a variety of conditions. The possibility that these changes in hydration of the matrix are associated with reversible movements of osmotically active components such as ions deserves consideration. Finally, our results indicate that structural damage may cause a slight increase in the equilibrium density of the mitochondria in a

sucrose gradient. In earlier studies made with the SW-39 rotor, a more extensive increase of this type has been observed; it could be evoked by exposure of the particles to high sucrose concentrations, and was tentatively attributed to a partial loss of hydration water from the matrix (11). The swollen appearance of many of the mitochondria in the denser subfraction 14 suggests, as an alternative possibility, that damage to the inner membrane could be the phenomenon responsible for the change. This hypothesis, which is compatible with the model discussed by de Duve et al. (17, 19), could be tested experimentally.

The authors wish to express their gratitude to Dr. Miklós Müller for performing the isocitric dehydrogenase assays, to Dr. Jacques Berthet for his valuable help in the early stages of this work, to Dr. G. E. Palade for having put electron microscope facilities at their disposal, to Misses Magdeleine Debbaudt, Linda Margolin, Valerie Budelman, and Annette Arcario for their competent technical assistance. These investigations have been supported by grant No. GB-5796x from the National Science Foundation. F. Leighton is the holder of a 1964–67 postdoctoral fellowship of the Rockefeller Foundation. P. Baudhuin is Chargé de Recherches du Fonds National de la Recherche Scientifique. J. W. Coffey is the holder of a 1965–67 postdoctoral fellowship of the United States Public Health Service.

Received for publication 11 October 1967.

REFERENCES

1. ADAMS, D. H., and E. A. BURGESS. 1957. The effect of the degree of homogenization on the catalase activity of liver "homogenates." *Brit. J. Cancer.* **11**:310.
2. APPELMANS, F., R. WATTIAUX, and C. DE DUVE. 1955. Tissue fractionation studies. 5. The association of acid phosphatase with a special class of cytoplasmic granules in rat liver. *Biochem. J.* **59**:438.
3. BAUDHUIN, P., H. BEAUFAY, and C. DE DUVE. 1965. Combined biochemical and morphological study of particulate fractions from rat liver. *J. Cell Biol.* **26**:219.
4. BAUDHUIN, P., H. BEAUFAY, Y. RAHMAN-LI, O. Z. SELLINGER, R. WATTIAUX, P. JACQUES, and C. DE DUVE. 1964. Tissue fractionation studies. 17. Intracellular distribution of monoamine oxidase, aspartate aminotransferase, alanine aminotransferase, D-amino acid oxidase and catalase in rat liver tissue. *Biochem. J.* **92**:179.
5. BAUDHUIN, P., and J. BERTHET. 1967. Electron microscopic examination of subcellular fractions. II. Quantitative analysis of the mitochondrial population isolated from rat liver. *J. Cell Biol.* **35**:631.
6. BAUDHUIN, P., P. EVRARD, and J. BERTHET. 1967. Electron microscopic examination of subcellular fractions. I. Preparation of representative samples from suspensions of particles. *J. Cell Biol.* **32**:181.
7. BAUDHUIN, P., M. MÜLLER, B. POOLE, and C. DE DUVE. 1965. Non-mitochondrial oxidizing particles (microbodies) in rat liver and kidney and in *Tetrahymena pyriformis*. *Biochem. Biophys. Res. Commun.* **20**:53.
8. BEAUFAY, H. 1966. La centrifugation en gradient de densité (Thèse d'Agrégation de l'Enseignement Supérieur, Université Catholique de Louvain, Louvain, Belgium). Ceuterick S. A., Louvain, Belgium. 132 pp.
9. BEAUFAY, H., D. S. BENDALL, P. BAUDHUIN, and C. DE DUVE. 1959. Tissue fractionation studies. 12. Intracellular distribution of some dehydrogenases, alkaline deoxyribonuclease and iron in rat-liver tissue. *Biochem. J.* **73**:623.
10. BEAUFAY, H., D. S. BENDALL, P. BAUDHUIN, R. WATTIAUX, and C. DE DUVE. 1959. Tissue fractionation studies. 13. Analysis of mitochondrial fractions from rat liver by density-gradient centrifuging. *Biochem. J.* **73**:628.
11. BEAUFAY, H., P. JACQUES, P. BAUDHUIN, O. Z. SELLINGER, J. BERTHET, and C. DE DUVE. 1964. Tissue fractionation studies. 18. Resolution of mitochondrial fractions from rat liver into three distinct populations of cytoplasmic particles by means of density equilibration in various gradients. *Biochem. J.* **92**:184.
12. BOWERS, W. E., and C. DE DUVE. 1967. Lysosomes in lymphoid tissue. II. Intracellular distribution of acid hydrolases. *J. Cell Biol.* **32**:339.
13. BUCHER, N. L. R. 1959. *In* Ciba Foundation Symposium on the Biosynthesis of Terpenes and Sterols. A. V. S. de Reuck and M. P. Cameron, editors. J. & A. Churchill, Ltd. London, 46.
14. CHANCE, B. 1950. The reactions of catalase in the presence of the notatin system. *Biochem. J.* **46**: 387.
15. CHANTRENNE, H. 1955. Effets d'un inhibiteur de la catalase sur la formation induite de cet enzyme chez la levure. *Biochim. Biophys. Acta.* **16**:410.
16. COOPERSTEIN, S. J., and A. LAZAROW. 1951. A

microspectrophotometric method for the determination of cytochrome oxidase. *J. Biol. Chem.* **189**:665.

17. DE DUVE, C. 1965. The separation and characterization of subcellular particles. *Harvey Lectures.* Ser. **59**:49.
18. DE DUVE, C., and P. BAUDHUIN. 1966. Peroxisomes (Microbodies and related particles). *Physiol. Rev.* **46**:323.
19. DE DUVE, C., J. BERTHET, and H. BEAUFAY. 1959. Gradient centrifugation of cell particles. Theory and applications. *Progr. Biophys. Biophys. Chem.* **9**:325.
20. DE DUVE, C., J. BERTHET, H. G. HERS, and L. DUPRET. 1949. Le système hexose-phosphatasique. I. Existence d'une glucose-6-phosphatase spécifique dans le foie. *Bull. Soc. Chim. Biol.* **31**:1242.
21. DE DUVE, C., B. C. PRESSMAN, R. GIANETTO, R. WATTIAUX, and F. APPELMANS. 1955. Tissue fractionation studies. 6. Intracellular distribution patterns of enzymes in rat-liver tissue. *Biochem. J.* **60**:604.
22. DELBRÜCK, A., H. SCHIMASSEK, K. BARTSCH, and T. BÜCHER. 1959. Enzym-verteilungsmuster in einigen Organen und in experimentellen Tumoren der Ratte und der Maus. *Biochem. Z.* **331**:297.
23. DETER, R. L., and C. DE DUVE. 1967. Influence of glucagon, an inducer of cellular autophagy, on some physical properties of rat liver lysosomes. *J. Cell Biol.* **33**:437.
24. FISKE, C. H., and Y. SUBBAROW. 1925. The colorimetric determination of phosphorus. *J. Biol. Chem.* **66**:375.
25. FRANTZ, I. D., AND B. T. HINKELMAN. 1955. Acceleration of hepatic cholesterol synthesis by Triton WR-1339. *J. Exptl. Med.* **101**:225.
26. GASS, S. I. 1958. Linear Programming. McGraw-Hill Book Company, New York.
27. HACKENBROCK, C. R. 1966. Ultrastructural bases for metabolically linked mechanical activity in mitochondria. I. Reversible ultrastructural changes with change in metabolic steady state in isolated liver mitochondria. *J. Cell Biol.* **30**:269.
28. HESS, R., W. STÄUBLI, and W. RIESS. 1965. Nature of the hepatomegalic effect produced by ethyl-chlorophenoxyisobutyrate in the rat. *Nature.* **208**:856.
29. HOGEBOOM, G. H., and W. C. SCHNEIDER. 1950. Cytochemical studies of mammalian tissues. III. Isocitric dehydrogenase and triphosphopyridine nucleotide-cytochrome *c* reductase of mouse liver. *J. Biol. Chem.* **186**:417.
30. HOGEBOOM, G. H., AND W. C. SCHNEIDER. 1953. Intracellular distribution of enzymes. XI. Glutamic dehydrogenase. *J. Biol. Chem.* **204**: 233.
31. HORECKER, B. L. and A. KORNBERG. 1948. The extinction coefficients of the reduced band of pyridine nucleotides. *J. Biol. Chem.* **175**:385.
32. HRUBAN, A., and H. SWIFT. 1964. Uricase: Localization in microbodies. *Science.* **146**:1316.
33. KALCKAR, H. M. 1947. Differential spectrophotometry of purine compounds by means of specific enzymes. I. Determination of hydroxypurine compounds. *J. Biol. Chem.* **167**:429.
34. KORNBERG, A. 1955. Isocitric dehydrogenase of yeast (TPN). *In* Methods in Enzymology. S. P. Colowick and N. O. Kaplan, editors. Academic Press, Inc., New York. **1**:705.
35. LOUD, A. V., W. C. BARANY, and B. A. PACK. 1965. Quantitative evaluation of cytoplasmic structures in electron micrographs. *Lab. Invest.* **14**:996.
36. LOWRY, O. H., N. J. ROSEBROUGH, A. L. FARR, and R. J. RANDALL. 1951. Protein measurement with the Folin phenol reagent. *J. Biol. Chem.* **193**:265.
37. ROSIWAL, A. 1898. Über geometrische Gesteinanalysen. *Verhandl. k.k. geologischen Reichsanstalt, Wien*:143.
38. SAWANT, P. L., S. SHIBKO, U. S. KUMTA, and A. L. TAPPEL. 1964. Isolation of rat-liver lysosomes and their general properties. *Biochim. Biophys. Acta.* **85**:82.
39. SCANU, A., and P. ORIENTE. 1961. Triton hyperlipemia in dogs. I. In vitro effects of the detergent on serum lipoproteins and chylomicrons *J. Exptl. Med.* **113**:735.
40. SCHNEIDER, W. C., and G. H. HOGEBOOM. 1952. Intracellular distribution of enzymes. IX. Certain purine-metabolizing enzymes. *J. Biol. Chem.* **195**:161.
41. SELLINGER, O. Z., H. BEAUFAY, P. JACQUES, A. DOYEN, and C. DE DUVE. 1960. Tissue fractionation studies. 15. Intracellular distribution and properties of β-N-acetylglucosaminidase and β-galactosidase in rat liver. *Biochem. J.* **74**:450.
42. SHEPHERD, J. A., and G. KALNITSKY. 1954. Intracellular distribution of fumarase, aconitase, and isocitric dehydrogenase in rabbit cerebral cortex. *J. Biol. Chem.* **207**:605.
43. SHNITKA, T. K. 1966. Comparative ultrastructure of hepatic microbodies in some mammals and birds in relation to species differences in uricase activity. *J. Ultrastruct. Res.* **16**:598.
44. SMITH, C. S., and L. GUTTMAN. 1953. Measurement of internal boundaries in three-dimensional structures by random sectioning. *J. Metals.* **5**:81.
45. SVOBODA, D. J., and D. L. AZARNOFF. 1966. Response of hepatic microbodies to a hypo-

lipidemic agent, ethyl chlorophenoxyisobutyrate (CPIB). *J. Cell Biol.* **30**:442.

46. SWICK, R. W., J. L. STANGE, S. L. NANCE, and J. F. THOMSON. 1967. The heterogeneous distribution of mitochondrial enzymes in normal rat liver. *Biochemistry*. **6**:737.
47. TROUET, A. 1964. Immunisation de lapins par des lysosomes hépatiques de rats traités au Triton WR-1339. *Arch. Intern. Physiol. Biochim.* **72**:698.
48. TSUKADA, T., Y. MOCHIZUKI, and S. FUJIWARA. 1966. The nucleoids of rat liver cell microbodies. *J. Cell Biol.* **28**:449.
49. VAN DEN BOSCH, J., E. EVRARD, A. BILLIAU, P. DE SOMER, and J. V. JOOSSENS. 1961. The influence of a new *p-tert*-octylphenol derivative on the clearing factor and on the plasma lipids of rabbits. *J. Atherosclerosis Res.* **1**:148.
50. WATTIAUX, R. 1966. Etude expérimentale de la surcharge des lysosomes. (Thèse d'Agrégation de l'Enseignement Supérieur, Université Catholique de Louvain, Louvain, Belgium). Imprimerie J. Duculot, Gembloux, Belgium. 149pp.
51. WATTIAUX, R., M. WIBO, and P. BAUDHUIN. 1963. Influence of the injection of Triton WR-1339 on the properties of rat-liver lysosomes. *In* Ciba Foundation Symposium on Lysosomes. A. V. S. de Reuck and M. P. Cameron, editors. J. &. A. Churchill, Ltd., London. 176.